Circulation Research

ORIGINAL RESEARCH

Effects of Atrial Fibrillation on the Human Ventricle

Steffen Pabel, Maria Knierim, Thea Stehle, Felix Alebrand, Michael Paulus, Marcel Sieme, Melissa Herwig, Friedrich Barsch, Thomas Körtl, Arnold Pöppl, Brisca Wenner, Senka Ljubojevic-Holzer, Cristina E. Molina, Nataliya Dybkova, Daniele Camboni, Thomas H. Fischer, Simon Sedej, Daniel Scherr, Christof Schmid, Christoph Brochhausen, Gerd Hasenfuß, Lars S. Maier, Nazha Hamdani, Katrin Streckfuss-Bömeke, Samuel Sossalla

RATIONALE: Atrial fibrillation (AF) and heart failure often coexist, but their interaction is poorly understood. Clinical data indicate that the arrhythmic component of AF may contribute to left ventricular (LV) dysfunction.

OBJECTIVE: This study investigates the effects and molecular mechanisms of AF on the human LV.

METHODS AND RESULTS: Ventricular myocardium from patients with aortic stenosis and preserved LV function with sinus rhythm or rate-controlled AF was studied. LV myocardium from patients with sinus rhythm and patients with AF showed no differences in fibrosis. In functional studies, systolic Ca^{2+} transient amplitude of LV cardiomyocytes was reduced in patients with AF, while diastolic Ca^{2+} levels and Ca^{2+} transient kinetics were not statistically different. These results were confirmed in LV cardiomyocytes from nonfailing donors with sinus rhythm or AF. Moreover, normofrequent AF was simulated in vitro using arrhythmic or rhythmic pacing (both at 60 bpm). After 24 hours of AF-simulation, human LV cardiomyocytes from nonfailing donors showed an impaired Ca^{2+} transient amplitude. For a standardized investigation of AF-simulation, human iPSC-cardiomyocytes were tested. Seven days of AF-simulation caused reduced systolic Ca^{2+} transient amplitude and sarcoplasmic reticulum Ca^{2+} load likely because of an increased diastolic sarcoplasmic reticulum Ca^{2+} leak. Moreover, cytosolic Na^{+} concentration was elevated and action potential duration was prolonged after AF-simulation. We detected an increased late Na^{+} current as a potential trigger for the detrimentally altered Ca^{2+}/Na^{+}-interplay. Mechanistically, reactive oxygen species were higher in the LV of patients with AF. CaMKII (Ca^{2+}/calmodulin-dependent protein kinase IIδc) was found to be more oxidized at Met281/282 in the LV of patients with AF leading to an increased CaMKII activity and consequent increased RyR2 phosphorylation. CaMKII inhibition and ROS scavenging ameliorated impaired systolic Ca^{2+} handling after AF-simulation.

CONCLUSIONS: AF causes distinct functional and molecular remodeling of the human LV. This translational study provides the first mechanistic characterization and the potential negative impact of AF in the absence of tachycardia on the human ventricle.

GRAPHIC ABSTRACT: A graphic abstract is available for this article.

Key Words: atrial fibrillation ■ calcium-calmodulin-dependent protein kinase type 2 ■ excitation contraction coupling ■ heart failure ■ oxidative stress

In This Issue, see p 959 | Meet the First Author, see p 961 | Editorial, see p 1011

Atrial fibrillation (AF) and heart failure (HF) often coexist in patients and are associated with worsened cardiovascular outcomes.[1–4] The CASTLE-AF trial demonstrated that rhythm control via catheter ablation may reduce mortality, HF hospitalization, and may improve left ventricular (LV) function in patients with HF with reduced ejection fraction and concomitant AF.[5] Early rhythm control improved cardiovascular outcomes in patients with AF lasting ≤1 year as recently demonstrated in the EAST-AFNET 4 trial.[6] Also, other previous

Correspondence to: Samuel Sossalla, MD, Universitätsklinikum Regensburg, Klinik für Innere Medizin II, Herzzentrum Regensburg, Franz-Josef-Strauß-Allee 11, 93053 Regensburg, Germany. Email samuel.sossalla@ukr.de

Supplemental Material is available at https://www.ahajournals.org/doi/suppl/10.1161/CIRCRESAHA.121.319718.
For Sources of Funding and Disclosures, see page 1008.

Circulation Research is available at www.ahajournals.org/journal/res

Novelty and Significance

What Is Known?

- Atrial fibrillation (AF) has been broadly investigated in the atria, but little is known about its effects on the left ventricle (LV).
- In patients with AF, rhythm control therapy is increasingly seen as a better strategy than ventricular rate control alone.
- However, the effects and mechanisms of nontachycardic AF on the human LV remain unclear.

What New Information Does This Article Contribute?

- LV cardiomyocytes from patients with preserved LV function and AF had an impaired cardiomyocyte excitation-contraction coupling with reduced systolic Ca^{2+} release.
- In vitro AF-simulation confirmed this detrimental phenotype with impaired Ca^{2+} handling, prolonged action potentials, and enhanced late Na^{+} current in primary cultures of human cardiac myocytes and iPSC-cardiomyocytes. While myocardial fibrosis and apoptosis remained unchanged, occurrence of reactive oxygen species was increased in the AF LV.
- We revealed that reactive oxygen species-dependent activation of Ca^{2+}/calmodulin-dependent protein kinase IIδc contributes to adverse remodelling of the AF LV.

AF and LV dysfunction very frequently coexist. Arrhythmias are known to eventually cause systolic LV dysfunction. Based on recent clinical trials, treatment strategies for patients with AF are increasingly focused on rhythm control compared with rate control therapy. However, the effects of AF on LV function remain unclear. Our study investigated the effects of AF on the human ventricle to provide pathophysiological understanding of the detrimental interaction between AF and LV function. This translational investigation included different patient cohorts and prospective validations using isolated adult human cardiomyocytes and human iPSC-cardiomyocytes. We could demonstrate that AF by itself in the absence of tachycardia causes impaired excitation-contraction coupling associated with increased levels of reactive oxygen species and CaMKII-dependent depression of systolic Ca^{2+} release. Thus, we provide an explanation for the clinically frequently observed deleterious interaction of AF and LV function. Besides that, our findings may provide a mechanistic rationale for the outcomes of recent clinical trials comparing rhythm and ventricular rate control. The harmful interaction between AF and LV function may spur scientists and clinicians to understand AF as a disease of the entire heart.

Nonstandard Abbreviations and Acronyms

AF	atrial fibrillation
AIP	autocamtide-2-related inhibitory peptide
AS	aortic stenosis
CaMKII	Ca^{2+}/calmodulin-dependent protein kinase IIδc
EF	ejection fraction
HF	heart failure
I_{NaL}	late Na^{+} current
iPSC-CM	human induced pluripotent stem cell cardiomyocyte
LV	left ventricular
NAC	N-acetylcysteine
NCX	Na^{+}-Ca^{2+} exchanger
PLB	phospholamban
RYR2	ryanodine-receptor type 2
SERCA2a	sarcoplasmic reticulum Ca^{2+} ATPase 2a
SR	sinus rhythm
TNT	troponin T

trials in patients with AF suggested beneficial effects of rhythm control therapy on cardiac function and other functional outcomes.[7] Even in patients with permanent AF with narrow QRS complex who were hospitalized for HF within the last year, ablation of the atrioventricular junction together with biventricular pacing significantly reduced mortality.[8] Based on recent clinical evidence such as the EAST-AFNET 4 trial, treatment strategies for patients with AF are increasingly focused on rhythm control therapy.[6,9]

Notably, restoration of sinus rhythm (SR) was shown to be superior to rate control in achieving contractile ventricular recovery in patients with HF and AF, indicating that the arrhythmic component of AF by itself may impact LV function and remodeling.[10,11] While the mechanisms of AF have been broadly investigated in the atria, the effects of AF on ventricular function are poorly understood.[2,12,13] Remarkably, even less is known about the pathophysiological consequences of nontachycardic AF with arrhythmic excitation of the human LV, despite being a very frequent scenario in daily clinical practice.

Clinical data reported adverse hemodynamic effects upon irregular pacing,[14] altered myocardial perfusion,[15]

or an increase in sympathetic nerve activity in patients with AF.[16] However, appropriate models suitable for studying mechanistic effects of arrhythmic ventricular excitation are scarce as in vivo models are limited by artificial pacing, while in vitro investigation of human tissue is challenging. Studies in neonatal rat cardiomyocytes suggested that irregular pacing of isolated cardiomyocytes can result in elevated oxidative stress,[17] induction of profibrotic pathways[17] and disturbed Ca^{2+} homeostasis.[18,19]

As rate control has often been regarded equivalent to rhythm control, it is of utmost clinical importance to understand the effects of arrhythmia per se on LV function. Therefore, we investigated the effects of AF on ventricular function utilizing human ventricular myocardium from patients with rate-controlled AF or SR with preserved LV function. Moreover, to prospectively investigate the effects of an arrhythmic cardiomyocyte excitation in a standardized manner, we studied chronically paced adult human cardiomyocytes as well as human induced pluripotent stem cell cardiomyocytes (iPSC-CMs).

METHODS

Data Availability

The data that support the findings of this study are available from the corresponding author upon reasonable request.

Patients

All procedures were performed according to the Declaration of Helsinki and were approved by the local ethics committee of the University of Regensburg (ref. no 20-1776-101), University of Göttingen (ref. no 10/9/15, 21/10/00 and 21/2/11) and Medical University of Graz (ref. no 28-508 ex 15/16). Informed consent was obtained from all patients. LV myocardium from patients with aortic stenosis (AS) undergoing surgical aortic valve replacement and septal resection (compensated hypertrophy) was acquired. Patients with SR or persistent/permanent rate-controlled AF with preserved systolic LV function as indicated by an echocardiographic EF≥50% were included. Moreover, human ventricular samples were additionally acquired from nonfailing donors (±AF), which could not be transplanted because of technical or medical reasons. Myocardial tissue was taken from the interventricular septum and immediately placed into cooled cardioplegic solution (4 °C) after excision for transportation. Patient characteristics are provided in Tables 1 and 2. Because of the limited amount of myocardial tissue, not all experimental methods could be performed from every patient sample.

Quantification of Myocardial Fibrosis

Tissue samples were fixed in neutral buffered formaldehyde (3.7%) and then embedded in paraffin according to standardized and automated methods (Sakura Fintek). Paraffin sections of 4 µm thickness and Elastica van Gieson staining were performed according to standardized methods. For semiautomated tissue analyses, whole slide images were performed by use of a scanner (M8 PreciPoint). Collagen proportionate area was analyzed (ImageJ with color threshold function to mark collagen fibers), blinded and semiautomated.

Table 1. Clinical Characteristics of Patients With AS and Preserved LV Function (EF>50%) Undergoing AVR With SR or AF

Characteristic (patients with AS)	SR (n=31 patients)	AF (n=24 patients)	*P* Value
Male sex, %	64.5	70.8	0.77 $_F$
Age, y (mean±SD)	66.2±8.5	72.5±8.0	0.01 $_T$*
White origin, %	100.0	100.0	0.99 $_F$
Heart rate, bpm (mean±SD)	73.1±13.0	79.0±18.4	0.41 $_{MW}$
Diabetes, %	27.6	33.3	0.77 $_F$
Coronary artery disease, %	51.9	59.1	0.77 $_F$
Ejection fraction, % (mean±SD)	57.1±3.4	55.8±5.0	0.34 $_{MW}$
IVS, mm (mean±SD)	13.8±2.4	13.6±2.5	0.92 $_{MW}$
AVA, cm^2 (mean±SD)	0.83±0.2	0.80±0.2	0.85 $_{MW}$
AV mean gradient, mm Hg (mean±SD)	43.7±16.3	36.3±11.6	0.12 $_T$
LVEDD, mm (mean±SD)	50.0±5.5	51.9±6.1	0.38 $_T$
ACE inhibitor or ARB, %	60.7	59.1	0.99 $_F$
β-blocker, %	53.6	73.9	0.16 $_F$
Aldosterone antagonist, %	8.0	10.0	0.99 $_F$
Diuretic, %	32.0	70.0	0.02 $_F$*
Digitalis, %	0.0	25.0	0.01 $_F$*
Antiarrhythmic, %	0.0	21.7	0.01 $_F$*
Statins, %	71.4	73.9	0.99 $_F$

Statistical comparison was calculated using Student *t* test for parametric data ($_T$), Mann-Whitney test *U* for nonparametric data ($_{MW}$), or Fisher exact test for categorical data ($_F$). Clinical data could not be completely obtained from every patient. Data are presented as mean±SD. ACE indicates angiotensin-converting enzyme; AF, atrial fibrillation; ARB, angiotensin II receptor blocker; AS, aortic stenosis; AV, aortic valve; AVA, aortic valve area; AVR, aortic valve replacement surgery; IVS, interventricular septum; LV, left ventricular; LVEDD, LV end-diastolic diameter; and SR, sinus rhythm.
*Significant *P*-values.

Isolation and Culture of Human Ventricular Cardiomyocytes

Ventricular myocardium was cleaned from fibrotic tissue and cut into small pieces in cardioplegic solution. For cell isolation, Joklik-MEM solution (Pan Biotech; pH 7.4 at 37 °C) was used. Cell isolation was started by incubating the tissue in enzyme solution containing 0.9 to 0.95 mg/mL Collagenase (Worthington type I, 315 U/mg), 0.23 mg/mL proteinase (Sigma-Aldrich, 7–14 U/mg) and 2 mg/mL BSA (BSA, Sigma-Aldrich) in a spinner flask. After 23 minutes, tissue was transferred to enzyme solution containing 0.58 mg/mL collagenase and 2.67 mg/mL BSA in a spinner flask and incubated for another 5 to 10 minutes. Then, the supernatant containing isolated cells was removed, and the remaining tissue was sheared mechanically in Joklik-MEM solution containing 5 mg/mL BSA to further solve cells. After centrifugation (RCF: 81.63 g, 5 minutes), the cells were resuspended in Joklik-MEM solution containing 5 mg/mL BSA. This procedure was repeated 5 to 8 times with the remaining tissue.[20] Ca^{2+} concentration was stepwise increased to 0.8

Table 2. Clinical Characteristics of LV Myocardium From Nonfailing Donors With SR or AF

Characteristic (nonfailing donors)	Sinus rhythm (n=18 patients)	Atrial fibrillation (n=10 patients)	*P* Value
Male sex, %	44.4	40.0	0.99 $_F$
Age, y (mean±SD)	68.6±8.2	69.5±10.6	0.80 $_T$
Ejection fraction, % (mean±SD)	62.5±5.9	61.2±6.8	0.63 $_T$

Statistical comparison was calculated using Student *t* test for parametric data ($_T$), Mann-Whitney *U* test for nonparametric data ($_{MW}$), or Fisher exact test for categorical data ($_F$). Clinical data could not be completely obtained from every patient. Data are presented as mean±SD. AF indicates atrial fibrillation; LV, left ventricular; and SR, sinus rhythm.

mmol/L after cell isolation. LV cardiomyocytes from large myocardial samples (>1 g) from donor hearts were isolated using 0.6 mg/mL collagenase Type 5 (Worthington) and 2.5% trypsin (Gibco) for 45 minutes and the second enzyme solution contained 1 mg/mL collagenase Type 5. Only cell solutions containing elongated, nongranulated cardiomyocytes with cross-striations were selected for experiments. Cardiomyocytes were used either for direct experiments or for cell culture (24 hours arrhythmic pacing for AF-simulation). For cell culture (37 °C, 5% CO_2), 2 mL of MEM-Medium (Gibco) containing 0.5 mg/mL Pen/Strep 100X (Gibco), 1% Insulin-Transferrin 100X (Gibco), 2 mmol/L L-Glutamin 100X (Gibco), 0.505 mg/mL BDM (Alfa Aesar), 0.1% BSA (Thermo Fisher Scientific) were mixed with 200 µL cell solution.

IPSC-Cardiomyocyte Differentiation

IPSCs were cultured feeder-free and adherent on cell culture dishes in the presence of chemically defined medium E8 (Life Technologies). Cardiac differentiation of iPSCs was performed by sequential targeting of the WNT pathway as described previously.[21] Briefly, undifferentiated iPSCs were cultured as a monolayer on Geltrex-coated 12-well dishes to a confluence of 85% to 95%. Medium was changed to cardio differentiation medium composed of RPMI 1640 medium (Gibco) supplemented with 0.02% L-Ascorbic Acid 2-Phosphate (Sigma-Aldrich) and 0.05% albumin (Sigma-Aldrich) including the GSK3 inhibitor CHIR99021 (4 µmol/L, Millipore) (d0). After 48 hours, medium was changed to fresh media supplemented with 5 µmol/L of the inhibitor of Wnt production-2 (IWP2, Millipore) for 2 days. From day 10, the cells were cultured in cardio culture medium (RPMI 1640 medium supplemented with 2 mmol/L l-glutamine and 2% B27 with insulin (Gibco), which was changed every 2 to 3 days. iPSC-CMs were purified after 20 to 40 days of differentiation by metabolic selection for 4 to 5 days using lactate (4 mmol/L) as carbon source. Following differentiation, purity of iPSC-CM was determined by Flow analysis (≈90% cardiac TNT$^+$), cardiac immunofluorescence, by morphology and qPCR for cardiac sub-type markers (Supplemental Material).[22] Measurements were performed around day 90 after initiation of differentiation. For functional experiments, iPSC-CMs were plated on glass dishes (World Precision Instruments). Because of technical reasons, not all 25 differentiations of iPSC-CMs were used for each functional assay.

Simulation of AF In Vitro

Isolated human ventricular cardiomyocytes or human iPSC-CM cultured in 6-well dishes were paced via electrical field stimulation using a culture stimulation system (C-Pace EM, IonOptix Corp.). Pacing was conducted for 24 hours (adult cardiomyocytes, iPSC-CM) or 7 days (iPSC-CM). Control cells were continuously stimulated at 60 beats per minute (bpm). AF was simulated via arrhythmic pacing at 60 bpm with irregular beat to beat intervals (40% variability). Stimulation pulse was set 10% to 20% above threshold to achieve a sufficient capture of the cells. Sufficient cell stimulation and cell viability were strictly and continuously monitored and reevaluated during cell culture and pacing.

Ca^{2+} Cycling Measurements

For the investigation of cardiomyocyte Ca^{2+} homeostasis, epifluorescence microscopy was used.[23] Cells were plated on laminin-coated chambers (adult cardiomyocytes) or gelatin-coated glass dishes (iPSC-CM) and were mounted on an inverted microscope (Nikon Eclipse TE2000-U). Cardiomyocytes were incubated with a Fura-2 AM loading buffer (Invitrogen), supplemented with Pluronic F-127 0.05% w/v (Sigma-Aldrich) for 15 minutes followed by 15 minutes incubation with Tyrode's solution (in mmol/l: NaCl 140, KCl 4, $MgCl_2$ 1, HEPES 10, Glucose 10, $CaCl_2$ 1.25 (iPSC-CM) or 2 (adult cardiomyocytes), pH 7.4, NaOH) to ensure de-esterification of intracellular Fura-2 before measurement was started. Fura-2 fluorescence ratio was calculated using alternating excitation at 340 and 380 nm. The emitted fluorescence was collected at 510 nm. Measurements were performed using a fluorescence detection system (IonOptix Corp.). Ca^{2+} transients were recorded at steady state conditions under constant rhythmic field stimulation (30–60 bpm) at room temperature. Sarcoplasmic Ca^{2+} content was assessed by caffeine application (10 mmol/L). SERCA2a (sarcoplasmic reticulum Ca^{2+} ATPase 2a) activity was estimated as difference between the decay constant K of the systolic Ca^{2+} transient and the caffeine-induced Ca^{2+} transient (K_{sys}-K_{caff}).[24] For CaMKII (Ca^{2+}/calmodulin-dependent protein kinase IIδc) inhibition, AIP (autocamtide-2-related inhibitory peptide, 1 µmol/L, Enzo) was used. N-acetylcysteine (NAC, 200 µmol/L, Sigma-Aldrich) was used as ROS-scavenger. Treatment was applied for 7 days during cell culture as well as during the functional measurements of iPSC-CM. The recorded Ca^{2+} transients were analyzed with the software IonWizard (IonOptix Corp.).

Analysis of Diastolic Sarcoplasmic Reticulum Ca^{2+} Sparks

For assessing diastolic sarcoplasmic reticulum Ca^{2+} sparks, iPSC-CMs were loaded with Fluo-4 AM (10 µmol/L, Invitrogen) in the presence of Pluronic F-127 0.05 % w/v (Life Technologies) for 15 minutes and then incubated with Tyrode's solution for 15 minutes.[25,26] Ca^{2+} spark measurements were performed at room temperature by using a laser scanning confocal microscope (LSM 7 Pascal, Zeiss). Fluo-4 was excited by an argon ion laser (488 nm), and emitted fluorescence was collected through a 505 nm long-pass emission filter. Fluorescence images were recorded in the line-scan mode (512 pixels per line, scan width: 35.4 µm, pixel time: 0.64 µs, 10 000 unidirectional line scans/image, 6.9-second

measurement period). Ca^{2+} sparks were recorded during rest, immediately after stopping continuous electric field stimulation (rhythmic, 30 bpm). Diastolic Ca^{2+} sparks were analyzed with the program SparkMaster for ImageJ. The Ca^{2+} spark frequency of each cell resulted from the number of sparks normalized to scan width and time (100 $\mu m^{-1}*s^{-1}$).

Intracellular Na^+ Imaging

To assess intracellular Na^+ concentration ($[Na^+]_i$), iPSC-CMs were stained with SBFI-AM 10 µmol/L (Invitrogen) and Pluronic F-127 0.05 % w/v (Thermo Fisher Scientific) for 90 minutes at room temperature. To allow de-esterification of the dye, cells were incubated for additional 20 minutes with Tyrode's solution. Cell culture dishes were mounted on a Nikon Eclipse TE-2000-U microscope equipped with a HyperSwitch Light Source and Fluorescence System Interface (both IonOptix). SBFI fluorescence ratio F_{340}/F_{380} was obtained by recording emitted fluorescence at 510±40 nm during dual excitation (340 and 380 nm alternating at 240 Hz). Cells were measured at steady-state conditions under constant field stimulation (30 bpm). Recorded data were analyzed using IonWizard (IonOptix Corp.). Each iPSC-CM differentiation underwent calibration of SBFI to analyze $[Na^+]_i$ as previously described.[27] Cells were superfused with increasing extracellular Na^+ concentrations (0–20 mmol/L) in the presence of strophanthidin 100 µmol/L and gramicidin 10 µmol/L (both Sigma-Aldrich) to record a calibration curve. The solutions with various Na^+ concentrations were prepared by mixing potassium-free calibration solution (in mmol/L: NaCl 30, Na-gluconat 115, HEPES 10, glucose 10, EGTA 2, pH 7.4 with TRIS) with Na^+-free solution (in mmol/L: KCl 30, K-gluconat 115, HEPES 10, glucose 10, EGTA 2, pH 7.4 with TRIS) in the appropriate proportion.

Action Potential Measurements

Cardiomyocytes were incubated with Tyrode's solution for 15 minutes before measurements were started. Microelectrodes (2–4 MΩ) were filled with (in mmol/L): K-Aspartate 122, KCl 8, NaCl 10, MgCl2 1, HEPES 10, Mg-ATP 5, LiGTP 0.3 (pH 7.2, KOH). Access resistance was typically <10 MΩ after rupture. For action potential recordings, whole-cell current-clamp technique was used (HEKA electronics).[25] Action potentials were continuously elicited by current pulses (0.75–1 nA, 2–6 ms) at 30 bpm at room temperature. Fast capacitance was compensated in cell-attached configuration. Membrane capacitance and series resistance were compensated after patch rupture. Signals were filtered with 2.9 and 10 kHz Bessel filters and recorded with an EPC10 amplifier (HEKA Elektronik). Recordings were analyzed using LabChart 8 (ADInstruments).

I_{NaL} Measurements

Ruptured-patch whole-cell voltage-clamp was used to measure I_{NaL} (HEKA electronics).[28] Microelectrodes (2–4 MΩ) were filled with (in mmol/L): CsCl 95, Cs-glutamate 40, NaCl 10, $MgCl_2$ 0.92, Mg-ATP 5, Li-GTP 0.3, HEPES 5, niflumic acid 0.03 (to block Ca^{2+}-activated chloride current), nifedipine 0.02 (to block Ca^{2+} current), strophanthidin 0.004 (to block Na^+/K^+-ATPase) EGTA 1, and $CaCl_2$ 0.36 (free $[Ca^{2+}]_i$,100 nmol/L, pH 7.2, CsOH). The bath solution contained (in mmol/L): NaCl 135, tetramethylammonium chloride 5, CsCl 4, $MgCl_2$ 2, glucose 10, HEPES 10 (pH 7.4, CsOH). Access resistance was <7 MΩ. Cardiomyocytes were held at −120 mV, and I_{NaL} was elicited using a train of pulses to −35 mV (1000 ms duration, 10 pulses, BCL 2s). Recordings were initiated 4 to 5 minutes after rupture and were performed at room temperature. The measured current was integrated (between 100 and 500 ms) and normalized to the membrane capacitance.

Western Blot

For protein expression and phosphorylation analysis, we used 6%, 12%, and 15% SDS-PAGE. The expression of RYR2 (ryanodine-receptor type 2), NCX (Na^+-Ca^{2+} exchanger), SERCA2a, PLB (phospholamban), and CaMKII was studied using specific antibodies anti-RyR2 (mouse monoclonal antibody, dilution 1:1000, Santa Cruz Biotechnology), NCX (mouse monoclonal antibody, dilution 1:1000, Swant), SERCA2a (rabbit polyclonal antibody, dilution 1:1000, Alomone), PLB (mouse monoclonal antibody, dilution 1:1000, Thermo Fisher) and CaMKII-δ (rabbit polyclonal antibody, dilution 1:1000, Thermo Fisher). The phosphorylation of RyR2 and CaMKII was studied using anti-phospho-RyR2 (S2814; rabbit polyclonal antibody, dilution 1:1000, Thermo Fisher) and anti-phospho-CaMKII (Thr286; rabbit monoclonal antibody, dilution 1:1000, Cell Signaling Technologies). The oxidation of CaMKII was studied using anti-oxidized-CaMKII (Met281/282; rabbit polyclonal antibody, dilution 1:1000, Genetex).

Samples were applied at a concentration that was within the linear range of the detection system: 20 µg (dry weight). After separation, proteins were transferred to Merck Millipore polyvinylidenflouride membranes (pore size 0.45 nm). Blots were preincubated with 5% BSA in Tween Tris-buffered saline (TBS-T: 10 mmol/L Tris-HCl pH 7.6, 75 mmol/L NaCl, 0.1% Tween) for one hour at room temperature. Then, blots were incubated overnight at 4°C with the primary antibodies against the respective (phospho-) protein. After washing with TBS-T, primary antibody binding was visualized using a secondary horseradish peroxidase-labeled, goat-anti-rabbit/mouse antibody (dilution 1:10 000; OriGene Technologies GmbH and Jackson ImmunoResearch Europe Ltd, respectively) and enhanced chemiluminescence (ECL Western blotting detection, Amersham Biosciences) on a Biorad ChemiDoc XRS. The signals were analyzed with Multi Gauge V3.2 and BioRad ImageLab V6.1 software. All signals of small proteins were normalized to GAPDH (dilution 1:10 000; Sigma) stained on the same blots.

Hydrogen Peroxide Emission

Stable H_2O_2 accumulation was assessed in myocardial homogenates using a colorimetric peroxidase assay kit (Sigma-Aldrich; MAK311).[29] Subsequently, 40 µL of each standard into wells of a 96-well plate was added to 40 µL of each sample into separate wells. Followed by 200 µL of prepared detection reagent to each sample and standard well. To initiate the reaction, it was incubated for 30 minutes at room temperature. Then, the absorbance was measured at 585 nm (A585).

To quantify hydrogen peroxide emission in iPSC-CM, the Amplex Red Hydrogen Peroxide/Peroxidase Assay Kit (Invitrogen) was used. Cell culture medium of iPSC-CM cultures was replaced with a working solution containing Amplex Red 50 µmol/L and horseradish peroxidase 0.1 U/mL. Simultaneously, a standard curve was prepared according to

the manufacturer's instructions. After incubation for 30 minutes, fluorescence of the working solution (excitation 530 nm, emission 590 nm) was measured.

CaMKII Activity Testing

CaMKII activity was determined using a CycLex CaMKII assay kit and MyBiosource according to the manufacturer's guidelines.[30] Briefly, frozen tissues were homogenized in sample buffer containing 15% glycerol, 62.5 mmol/L Tris; pH 6.8; 1% (w/v) SDS, protease inhibitor, and protein phosphatase inhibitor, all prepared in distilled H_2O or buffer provided by the kit according to the manufacturer's guidelines. Homogenates were centrifuged at 10000×*g* for 15 minutes at 4°C. The supernatant was removed and stored at −80°C. Protein samples were loaded to microwells coated with CaMKII specific substrate, syntide-2, along with kinase reaction buffer with or without Ca^{2+}/calmodulin. To quantify CaMKII activity, a standard curve correlating the amount of active CaMKII and the level of phosphorylation of syntide-2 was constructed.

Flow Cytometry for Apoptosis

To evaluate apoptosis in iPSC-CM after in vitro pacing, APC Annexin V Apoptosis Detection Kit (BioLegend) was used following the manufacturer's instructions. After dissociation from the culture plates, cells were resuspended in 100 µL Annexin V Binding Buffer with 5 µL of APC Annexin V and 10 µL propidium iodide solution, followed by incubation for 15 minutes at room temperature. After adding 400 µL Annexin V Binding Buffer, cells were analyzed by flow cytometry utilizing a BD FACSCalibur (BD Life Sciences) with dual excitation at 488 and 635 nm. Events were gated using CellQuest Pro 5 (BD Life Sciences) depending on APC and propidium iodide fluorescence intensity. Flow cytometry gates were set up using a positive control with staurosporine 1 mmol/L (Sigma-Aldrich). Apoptosis rate was calculated as the percentage of events positive for APC and negative for propidium iodide.

Statistics

Clinical data are expressed as mean values±SD. All experimental data are presented as mean values±SD. As individual observations (measurements of single cells) are dependent on each other within one heart/differentiation, the mean of each patient or iPSC-CM differentiation was calculated and used for statistical testing. Mean values of the patients or differentiations are provided in the scatter dot plot within the figure. The total numbers of analyzed cells, patients, and cardiac iPSC-CM differentiations are provided below each figure. Normal distribution of data was tested with the Shapiro-Wilk test if applicable. In datasets with sample sizes too small for normality testing, normality was extrapolated from control data pooled across experiments. Categorical data were analyzed using Fisher exact test. For comparison of 2 groups containing normally distributed data from different patients/differentiations unpaired Student *t* test was used. For analysis of 2 groups containing normally distributed data from the same patient or differentiation (±treatment with AF-simulation) paired *t* test was applied. For not normally distributed data, Mann-Whitney *U* test was used. Analysis of data sets including >2 groups was performed using nested 1-way ANOVA corrected for multiple comparisons using Holm-Sidak test. Graphpad Prism 9 was used for statistical analysis. *P* are 2-sided and considered statistically significant if $P<0.05$.

RESULTS

Patient Characteristics

LV myocardium was obtained from patients with AS with preserved systolic LV function undergoing aortic valve replacement. Clinical characteristics of patients with SR (n=31 patients) or AF (n=24) are provided in Table 1. While general characteristics and comorbidities were balanced, patients with AF were older (72.5±8.0 years) than patients with SR (66.2±8.5 years). As we aimed to evaluate the effects of AF per se in the absence of tachycardia, patients with AF were characterized by a preserved LV function with an echocardiographic EF of 55.8±5.0% and a heart rate of 79.0±18.4 bpm, both of which were not statistically different to SR patients (57.1±3.4%, 73.1±13.0 bpm). Importantly, echocardiographic measurements of the aortic valve area and the aortic valve mean pressure gradient demonstrated no difference in the severity of AS between the groups. Likewise, LV remodeling as indicated by the interventricular septum thickness and the LV-end diastolic diameter did not differ between AF and SR patients (Table 1). However, patients with AF received digitalis, diuretic therapy, and antiarrhythmic drugs more often (Table 1).

Moreover, LV myocardium was procured from nonfailing donors with SR (n=18 patients) or AF (n=10). Because of ethical and clinical reasons, availability of clinical data is generally limited. Clinical characteristics of nonfailing donors ± AF are presented in Table 2. Donors with AF showed no differences in sex and age compared with individuals with SR. Also, EF was not significantly different in donors with AF (61.2±6.8%) compared with SR (62.5±5.9%).

Ventricular Fibrosis in Patients With AF

Using the histochemical fiber staining Elastica van Gieson and blinded semiautomated tissue analyses, we found no statistical difference in the amount and distribution of fibrosis between SR and AF LV myocardium from patients with AS and preserved LV function (Figure 1A). The collagen proportionate area was 16.7±5.2% in myocardium from patients with SR (n=10 patients) compared with 13.6±6.0% in AF (n=13 patients, Figure 1B).

AF Impairs Systolic Ca^{2+} Release in the Human Ventricle

For functional investigation, we isolated human LV cardiomyocytes from patients with preserved LV function with SR or AF. As Ca^{2+} handling is a major regulator of cardiac contractility, we studied cellular Ca^{2+} cycling using

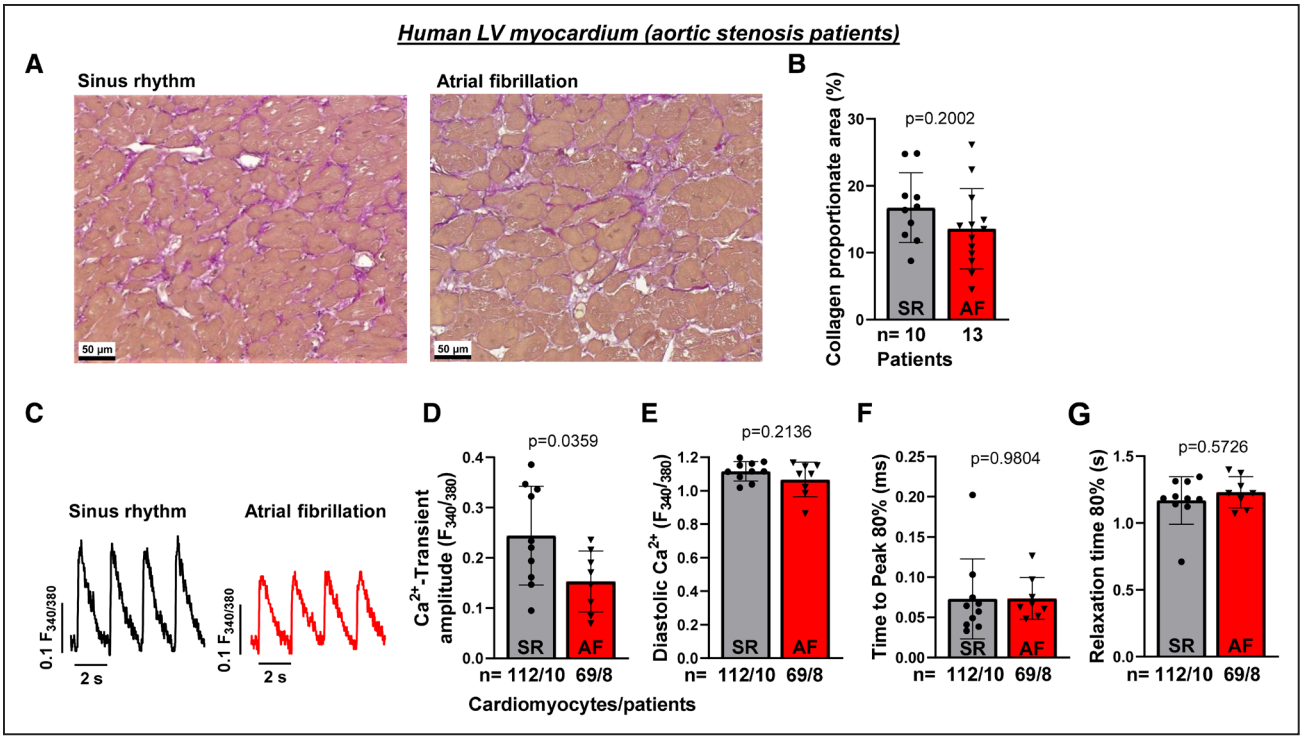

Figure 1. Fibrosis and Ca^{2+} handling in the atrial fibrillation (AF) ventricle.
Human left ventricular (LV) myocardium was studied from patients with aortic stenosis (AS) with preserved LV function with sinus rhythm (SR) or AF (clinical characteristics are given in Table 1). **A**, Representative stainings (Elastica van Gieson) and (**B**) mean values for collagen proportionate area in ventricular SR (n=10 patients) and AF myocardium (n=13). **C**, Representative original recordings of stimulated Ca^{2+} transients (epifluorescence microscopy, Fura-2) of human LV cardiomyocytes from patients with SR or AF. **D**, Mean values of Ca^{2+} transient amplitude of human LV cardiomyocytes from patients with SR (n=112 cardiomyocytes/10 patients) compared with AF (n=69/8) and (**E**) diastolic Ca^{2+} levels, (**F**) time to peak 80%, (**G**) relaxation time 80%. Data are presented as scatter plot with mean±SD. Each data point represents the mean value of measurements from one patient. *P* were computed using Student *t* test.

epifluorescence microscopy (Fura-2, Figure 1C). Isolated LV cardiomyocytes from patients with AF were characterized by a reduced Ca^{2+} transient amplitude (0.17±0.09 $F_{340/380}$, n=69 cardiomyocytes/8 patients) compared with cardiomyocytes from patients with SR (0.27±0.18 $F_{340/380}$, n=112/10, Figure 1D). Diastolic Ca^{2+} level and Ca^{2+} transient kinetics were not significantly changed in patients with AF (Figure 1E through 1G).

In addition, we investigated human ventricular myocardium from nonfailing donors. Comparing LV cardiomyocytes from donors, we also observed a reduced Ca^{2+} transient amplitude in AF cardiomyocytes (n=17 cardiomyocytes/4 nonfailing donors) compared with SR (n=46/8, Figure 2A and 2B), while diastolic Ca^{2+} level and Ca^{2+} transient kinetics showed no significant alterations (Figure 2C through 2E). As clinical characteristics may influence the observed phenotype, we conducted a standardized prospective normofrequent in vitro AF-simulation for 24 hours, which was compared with rhythmic pacing. Noteworthy, we used 24-hour cultured human LV cardiomyocytes from nonfailing donors for AF-simulation. Again, cardiomyocytes developed a significantly reduced Ca^{2+} transient amplitude after 24-hour arrhythmic pacing (n=43/8) compared with control (n=52/8, Figure 2F and 2G), while Ca^{2+} transient kinetics and diastolic Ca^{2+} levels were not significantly different (Figure 2H through 2J). Taken together, these translational data demonstrate impaired ventricular systolic Ca^{2+} release in response to AF and AF-simulation.

Human iPSC-CM Develop Altered Ca^{2+} and Na^{+} Homeostasis Upon AF-Simulation

For extended investigation of chronic AF-simulation in healthy cardiomyocytes, we utilized human iPSC-CM. Human ventricular iPSC-CMs from 5 healthy individuals were generated (n=25 differentiations in total) and analyzed regarding differentiation efficiency and purity. Ventricular iPSC-CM displayed well-organized striated patterns visualized by α-actinin and titin and were 89.7±3.0% cTNT positive ($cTNT^{+}$) (Figure S1A and S1B). Immunocytochemical staining of cardiac subtype-specific proteins showed that 70.0±3.5% of ventricular cells were stained positive for the ventricular isoform of myosin light chain 2 and negative for the atrial isoform of myosin light chain 2 ($MLC2V^{+}/MLC2A^{-}$, Figure S1C). Ventricular differentiation was confirmed on mRNA level by qPCR (Figure S1D).

Arrhythmic (AF-simulation) or rhythmic pacing protocols were conducted for 7 days using electrical field

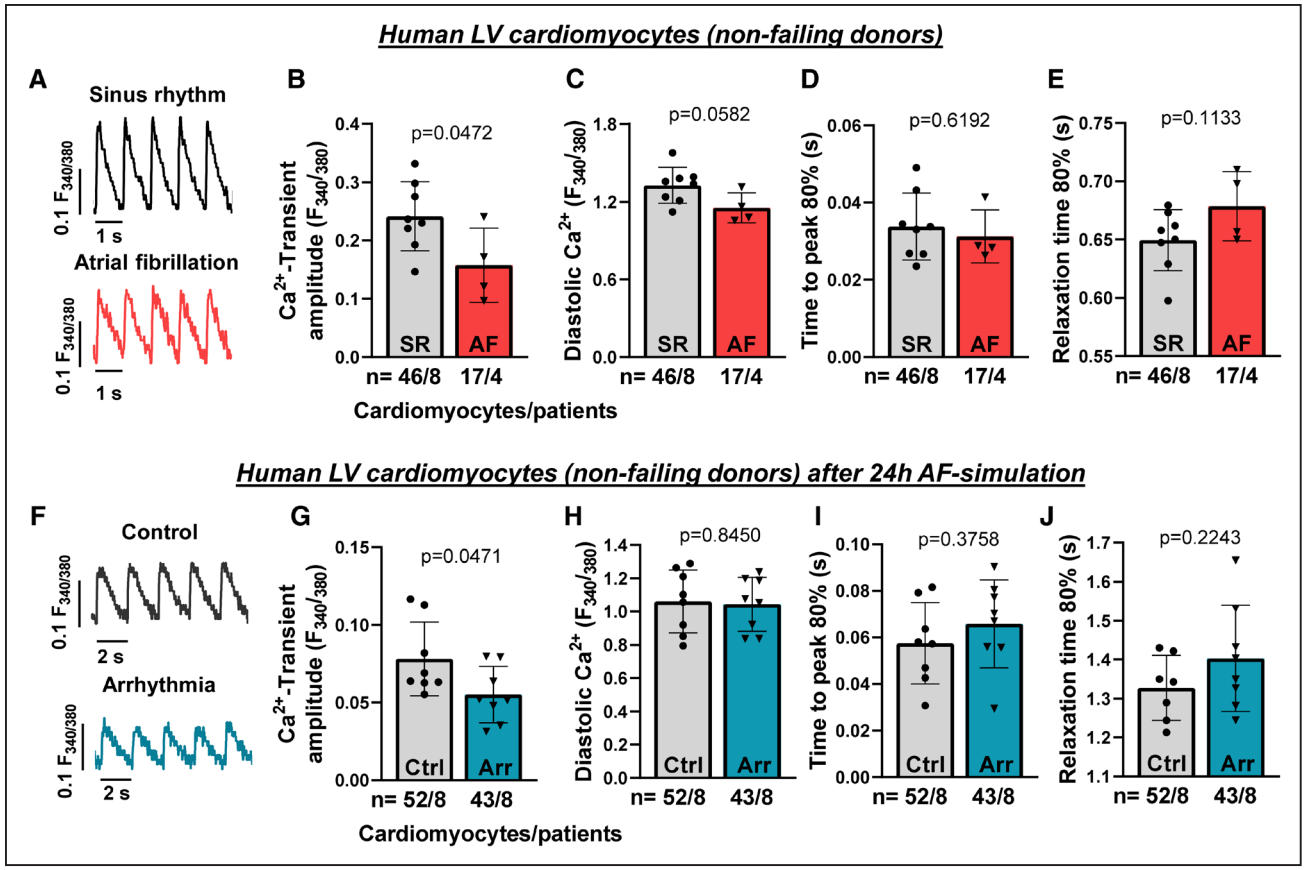

Figure 2. Effects of atrial fibrillation (AF) in human left ventricular (LV) myocardium from nonfailing donors.
A, Original Ca^{2+} transients from LV cardiomyocytes from nonfailing donors (clinical characteristics are provided in Table 2) with sinus rhythm (SR) or with AF (epifluorescence microscopy, Fura-2). **B**, Mean values of human LV cardiomyocytes from patients with SR (n=46 cardiomyocytes/8 patients) compared with AF (n=17/4) for Ca^{2+} transient amplitude, (**C**) diastolic Ca^{2+} level, (**D**) time to peak 80%, (**E**) relaxation time 80%. **F**, Original Ca^{2+} transients of human LV cardiomyocytes from nonfailing donors (epifluorescence microscopy, Fura-2) after 24-h in vitro AF-simulation (arrhythmic pacing: Arr; 60 bpm, 40% beat-to-beat variability) vs rhythmic pacing (control: Ctrl; 60 bpm). **G**, Mean values of human LV cardiomyocytes after AF-simulation (n=43/8) or rhythmic pacing (n=52/8) for Ca^{2+} transient amplitude, (**H**) diastolic Ca^{2+} level, (**I**) time to peak 80%, (**J**) relaxation time 80%. Data are presented as scatter plot with mean±SD. Each data point represents the mean value of measurements from one patient. *P* were calculated using Student *t* test.

stimulation (both at 60 bpm). After 7 days of AF-simulation, iPSC-CM exhibited a significantly reduced systolic Ca^{2+} transient amplitude (0.38±0.15 $F_{340/380}$, n=69 cardiomyocytes/6 differentiations/4 donors) in epifluorescence microscopy (Fura-2) compared with control (0.47±0.15 $F_{340/380}$, n=71/6/4, Figure 3A and 3B). Diastolic Ca^{2+} was not statistically altered (Figure 3C), and there were no significant changes in time to peak 80% (Figure 3D) and relaxation time 80% (Figure 3E) upon AF-simulation. In further mechanistic investigations, we detected a reduced sarcoplasmic reticulum Ca^{2+} load (caffeine application) in iPSC-CM after AF-simulation (0.73±0.15 $F_{340/380}$, n=13/6/4) compared with control (1.06±0.20 $F_{340/380}$, n=12/6/4, Figure 3F and 3G). SERCA2a activity (K_{sys}-K_{Caff}) was lower in arrhythmically paced iPSC-CM compared with control (Figure 3H). Of note, after 24 hours of AF-simulation, we found no statistical difference in systolic Ca^{2+} handling in iPSC-CM (Figure S2).

As sarcoplasmic reticulum Ca^{2+} load was reduced, we performed confocal microscopy measurements (Fluo-4) to investigate diastolic sarcoplasmic reticulum Ca^{2+} leak. iPSC-CM showed a >2-fold increased frequency of diastolic sarcoplasmic reticulum Ca^{2+} sparks after 7 days of AF-simulation (n=68/7/4) compared with control cells (n=67/7/4, Figure 3I and 3J). The reduction in sarcoplasmic reticulum Ca^{2+} load, likely caused by leaky RyR2, may explain the diminished systolic Ca^{2+} transient amplitude and constitutes a well-accepted key player for contractile dysfunction in HF.[31] Since Ca^{2+} handling is closely linked with cellular Na^+ homeostasis, we investigated alterations in cytosolic Na^+ via epifluorescence microscopy (SBFI). Cytosolic Na^+ in iPSC-CM was significantly elevated after arrhythmic pacing (n=110/7/4) compared with control (n=98/7/4, Figure 3K and 3L).

AF/AF-Simulation Prolongs the Ventricular Action Potential and Enhances I_{NaL}

Detailed electrophysiological studies were conducted to further clarify the mechanisms of LV remodeling

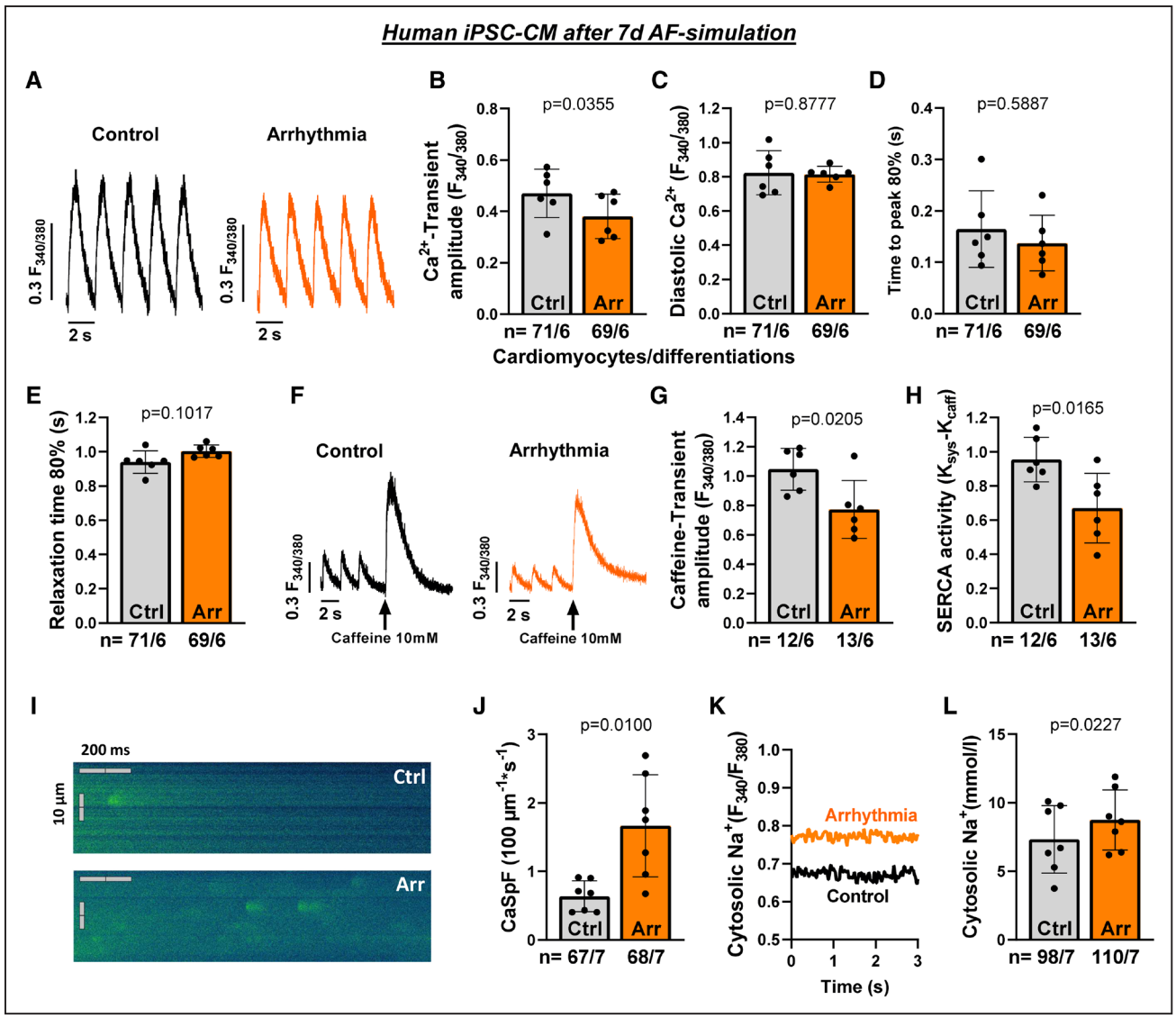

Figure 3. Atrial fibrillation (AF)-simulation in induced pluripotent stem cell cardiomyocytes (iPSC-CMs).
Human iPSC-CMs treated either with AF-simulation (arrhythmic pacing: Arr; 60 bpm, 40% beat-to-beat-variability) or rhythmic pacing (control [Ctrl]; 60 bpm) chronically for 7 d. **A**, Representative recordings of stimulated Ca^{2+} transients (epifluorescence microscopy, Fura-2) and (**B**) mean values for Ca^{2+} transient amplitude, (**C**) diastolic Ca^{2+} levels, (**D**) time to peak 80%, (**E**) relaxation time 80% of human iPSC-CM upon chronic AF-simulation (n=69 cardiomyocytes/6 differentiations/4 donors) or rhythmic pacing (n=71/6/4). **F**, Original recordings of caffeine-induced Ca^{2+} transients (10 mmol/l caffeine, epifluorescence microscopy, Fura-2), (**G**) mean caffeine-transient amplitude indicating the sarcoplasmic reticulum Ca^{2+} load and (**H**) SERCA2a activity (K_{sys}-K_{caff}) of iPSC-CM after chronic AF-simulation (n=13/6/4) vs control (n=12/6/4). **I**, Representative confocal line scans (Fluo-4) showing diastolic sarcoplasmic reticulum Ca^{2+} sparks and (**J**) mean Ca^{2+} spark frequency (CaSpF) after chronic AF-simulation (n=68/7/4) vs control (n=67/7/4). **K**, Original recordings of cytosolic Na^+ levels (epifluorescence microscopy, SBFI) and (**L**) mean values of cytosolic Na^+ concentration of human iPSC-CM after chronic AF-simulation (n=110/7/4) compared with control (98/7/4). Data are provided as scatter plot with mean±SD. Each data point is calculated as mean value per differentiation. *P* were calculated using Student *t* test (**A**–**C**, **E**–**L**) or Mann-Whitney *U* test (**D**).

upon AF/AF-simulation. In patch clamp experiments, we observed a significantly prolonged action potential duration (APD_{90}) in LV cardiomyocytes from AS-patients with AF and preserved LV function (376.8±166.1 ms n=30 cells/10 patients) compared with SR (257.0±112.7 ms, n=39/12, Figure 4A and 4B). Resting membrane potential or action potential amplitude were not statistically different (Figure 4C and 4D). These results could be confirmed in iPSC-CM after 7 days of AF-simulation (n=15–16 cells/4 differentiations/4 individuals each, Figure 4E through 4H). As a potential explanation for the prolonged action potential duration and the detrimentally altered Ca^{2+}/Na^+ interplay, we found in further ion-current measurements a significantly enhanced late Na^+ current (I_{NaL}) in iPSC-CM after AF-simulation (−192.5±61.1 A*ms/F, n=19/6/2) compared with control (−127.9±34.1 A*ms/F, n=21/6/2, Figure 4I and 4J). The increased I_{NaL} may perpetuate the vicious cycle of Na^+/Ca^{2+} dysregulation, which is also present in HF.[28,32]

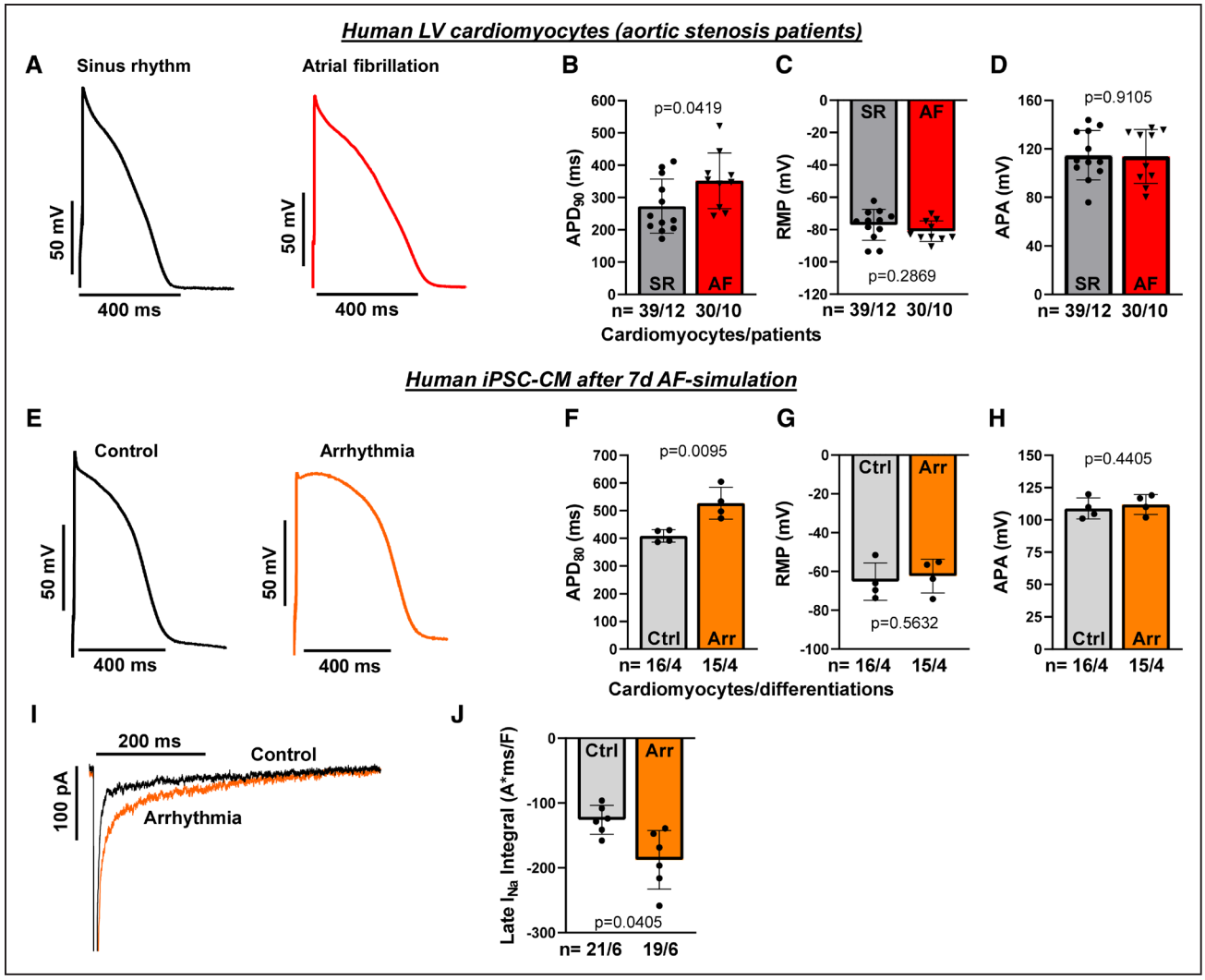

Figure 4. Electrophysiological alterations in response to atrial fibrillation (AF).
A, Original stimulated action potential recordings (whole-cell current-clamp) of human left ventricular (LV) cardiomyocytes from patients with aortic stenosis (AS) with preserved LV function with either sinus rhythm (SR) or AF. **B**, Effects of AF (n=30 cardiomyocytes/10 patients) compared with SR (n=39/12) on action potential (AP) duration at 90% repolarization (APD_{90}), **C**, Resting membrane potential (RMP) and (**D**) action potential amplitude (APA) in isolated human LV cardiomyocytes. **E**, Representative stimulated action potential recordings (whole-cell current-clamp) of iPSC-CM after chronic (7 d) AF-simulation (arrhythmic pacing: Arr; 60 bpm, 40% beat-to-beat-variability) compared with rhythmic pacing (control: ctrl; 60 bpm). **F**, Mean values for APD_{80}, (**G**) RMP and (**H**) APA after chronic AF-simulation (n=15 cardiomyocytes/4 differentiations/4 donors) compared with control (n=16/4/4). **I**, Original traces of late Na^+ current (I_{NaL}, whole-cell voltage-clamp) in iPSC-CM after chronic AF-simulation compared with control. **J**, Mean data of I_{NaL} (integral 100–500 ms) after AF-simulation (n=19/6/2) compared with control (n=21/6/2). Data are presented as scatter plot with mean±SD. Each data point is calculated as mean value per patient or differentiation. *P* were calculated using Student *t* test.

Remodeling of Ventricular EC-Coupling Proteins in AF

Western Blots of EC-coupling proteins were conducted using LV myocardium from patients with AS and preserved LV function. The total RyR2 protein expression was upregulated in the LV of AF patients (n=6–7 patients each, Figure 5A). In line with increased RyR2-mediated diastolic Ca^{2+} leak, RyR2 was hyperphosphorylated at the CaMKII-dependent RyR2 site S2814 in the AF ventricle compared with SR (n=6–7 patients each, Figure 5A and 5B). As RyR2 hyperphosphorylation increases the open probability (P_O) of the channel, these changes likely explain the increase in diastolic sarcoplasmic reticulum Ca^{2+} leak. Protein expression of the NCX, which mediates cytosolic Ca^{2+} removal in exchange with Na^+, was increased in the LV of patients with AF (n=6–7 patients each, Figure 5C). Also, SERCA2a expression was reduced in AF LV myocardium while PLB expression showed no statistical difference (n=6–7 patients each, Figure 5D and 5E).

Reactive Oxygen Species, CaMKII Oxidation, and CaMKII Activity in AF

To elucidate the mechanisms underlying EC-coupling protein remodeling in the LV of patients with AF, we

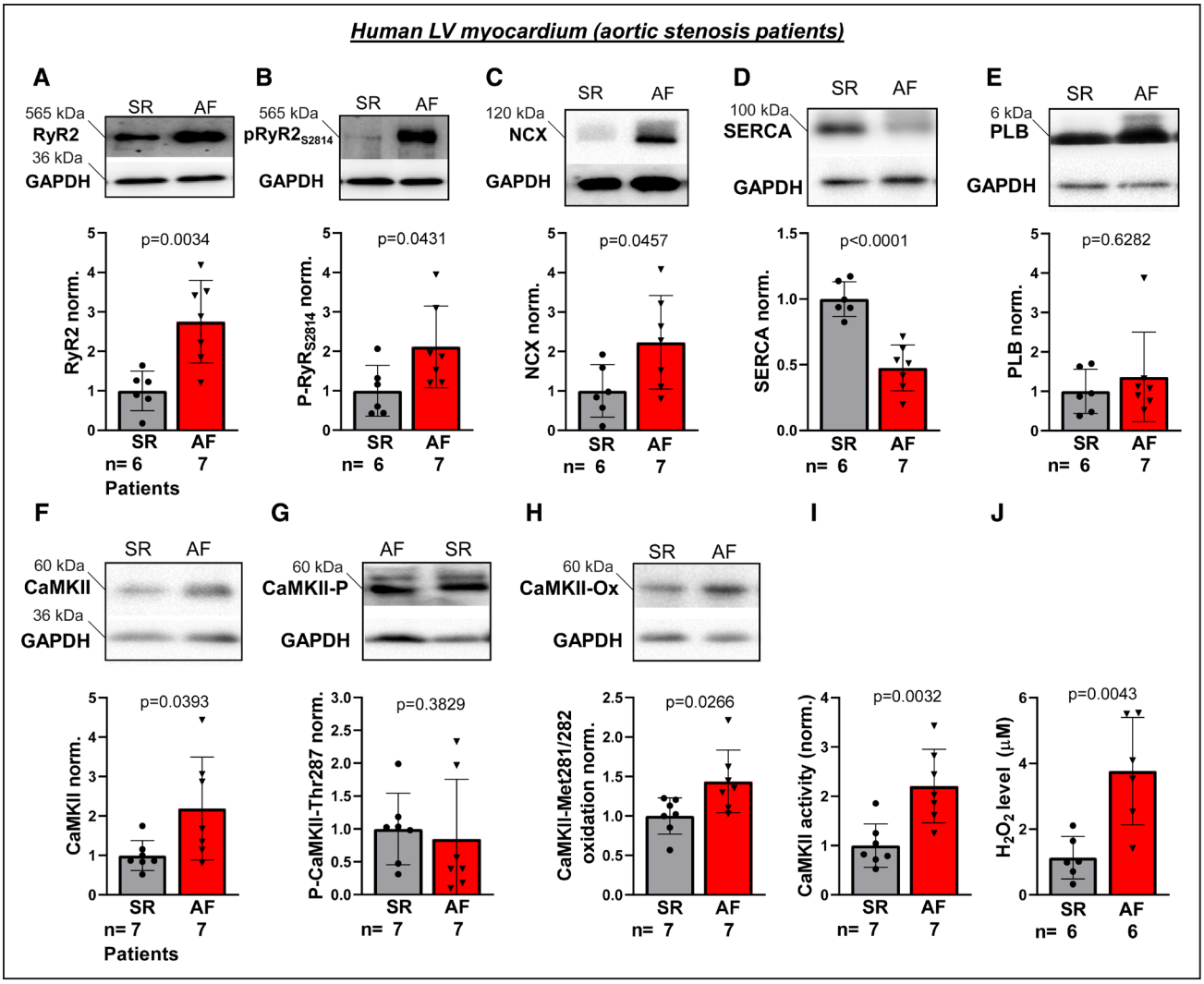

Figure 5. Molecular remodeling in the atrial fibrillation (AF) ventricle.
Original representative Western Blots of human left ventricular (LV) myocardium from aortic stenosis patients with preserved LV function with sinus rhythm (SR, n=6-7) or AF (n=7) and expression levels (normalized to SR) for (**A**) ryanodine receptor type 2 (RyR2), (**B**) RyR2 phosphorylation at Ser2814 (normalized to total RyR2 expression), (**C**) NCX (Na^+/Ca^{2+} exchanger), (**D**) SERCA (sarcoplasmic reticulum Ca^{2+} ATPase 2a), and (**E**) PLB (phospholamban). Representative Western Blots for (**F**) CaMKII (Ca^{2+}/calmodulin-dependent protein kinase IIδc), (**G**) CaMKII phosphorylation at Thr287 (CaMKII-P), and **(H)** CaMKII oxidation at Met281/282 (CaMKII-ox). GAPDH was used as loading control. **I**, CaMKII activity (CycLex CaMKII activity ELISA kit) and (**J**) H_2O_2 levels (colorimetric peroxidase assay) in LV myocardium from patients with SR or AF (n=6–7 each). Data are provided as scatter plot with mean±SD. Groups were statistically analysed using Student *t* test or Mann-Whitney *U* test (for **E** and **G**).

particularly investigated CaMKII regulation as it plays a central role for maladaptive remodeling in different cardiac diseases including HF. LV myocardium from AS patients with preserved LV function was studied. CaMKII expression was increased in patients with AF compared with SR patients (n=7 each, Figure 5F). CaMKII autophosphorylation at Thr287 was not significantly altered (Figure 5G). However, in patients with AF (n=7), CaMKII was found to be more oxidized at Met281/282 in the regulatory domain (Figure 5H), which has been demonstrated to activate CaMKII.[33] Accordingly, CaMKII activity was augmented in the LV of AF patients (n=7 each, Figure 5I). As oxidative stress contributes to CaMKII activity modulation, we measured the level of oxidative stress in the AF ventricle. LV myocardium from patients with AF (n=6) showed increased concentrations of hydrogen peroxide (H_2O_2) compared with SR patients (n=6, Figure 5J).

While overall CaMKII expression was not statistically different in iPSC-CM after chronic in vitro AF-simulation (n=4 differentiations/2 donors each, Figure 6A), CaMKII oxidation at Met281/282 was elevated (Figure 6B) resulting in increased CaMKII activity (Figure 6C). Increased levels of H_2O_2 after chronic in vitro AF-simulation (n=7 differentiations/3 donors each, Figure 6D) may underlie the oxidative CaMKII activation in iPSC-CM. Of note, the

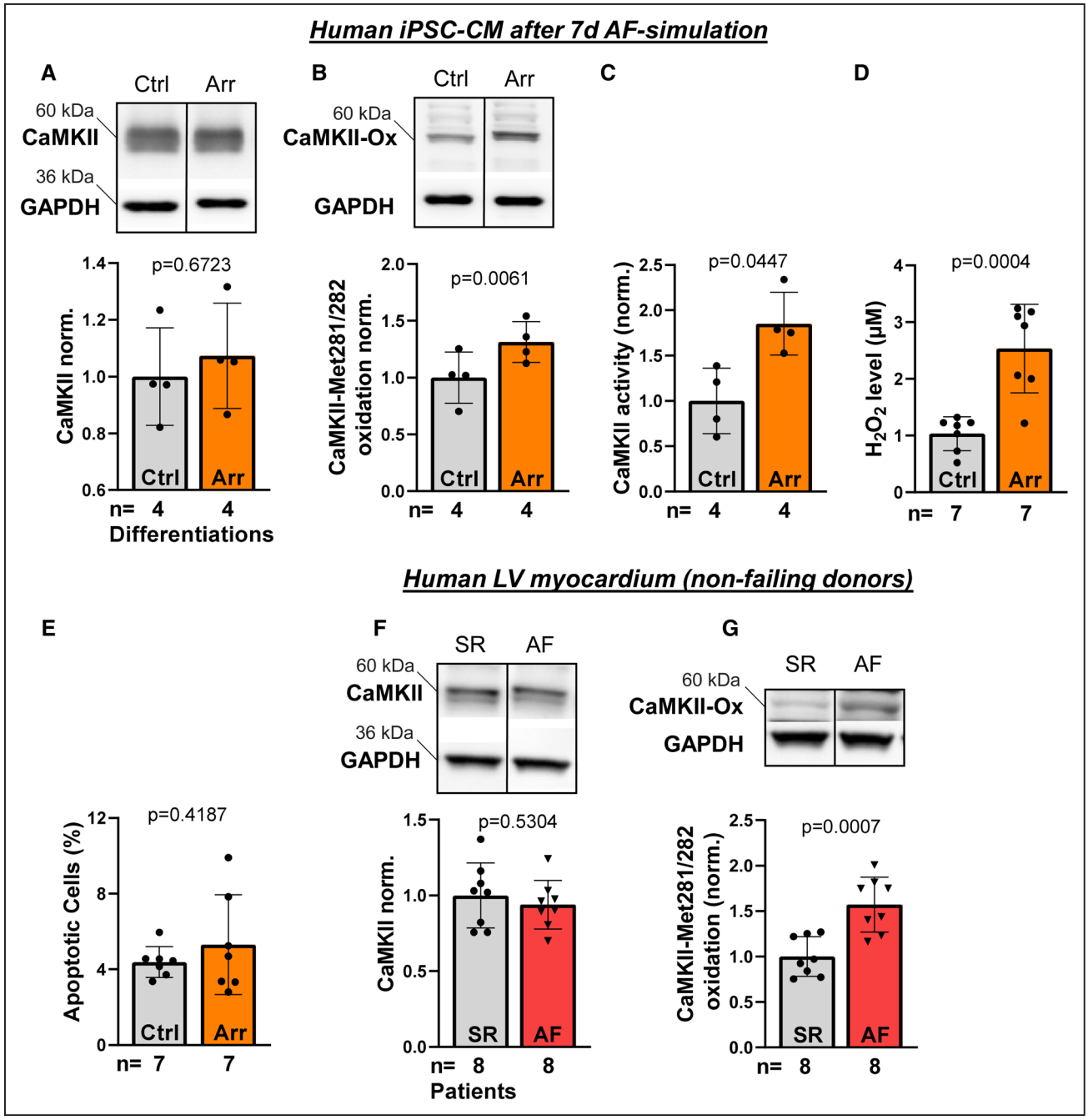

Figure 6. Molecular remodeling in response to atrial fibrillation (AF) in induced pluripotent stem cell cardiomyocytes (iPSC-CM) and in non-failing myocardium.

Original representative Western Blots of human iPSC-CMs after chronic (7 d) AF-simulation (Arr, n=4 differentiations/2 donors) or rhythmic pacing (control [Ctrl]; 60 bpm, n=4 differentiations/2 donors) and expression levels (normalized to SR) for (**A**) CaMKII (Ca^{2+}/calmodulin-dependent protein kinase IIδc) and (**B**) CaMKII oxidation at Met281/282 (CaMKII-ox). GAPDH was used as loading control. **C**, CaMKII activity (CycLex CaMKII activity ELISA kit, n=4 differentiations/2 donors each), (**D**) H_2O_2 levels (colorimetric peroxidase assay, n=7 differentiations/3 donors each) and (**E**) percentage of apoptotic cells (n=7 differentiations/3 donors each) in iPSC-CM after chronic (7 d) AF-simulation compared with control. **F**, Representative Western Blots for CaMKII and (**G**) CaMKII oxidation at Met281/282 (CaMKII-ox) in LV myocardium from nonfailing donors with SR or AF (n=6–7 donors each). GAPDH was used as loading control. All Blots were on the same respective gels but on different positions. Thus, membrane was cut (black middle line). Data are given as scatter plot with mean±SD. *P* were calculated using Student *t* test.

percentage of apoptotic cells (annexin V flow cytometry) was not statistically different in iPSC-CM after AF-simulation compared with control (n=7 differentiations/3 donors each, Figure 6E). Finally, increased CaMKII oxidation was also confirmed in human nonfailing myocardium from patients with AF compared with SR, while total CaMKII did not statistically differ (n=8 each, Figure 6F and 6G).

CaMKII Inhibition and ROS Scavenging Prevents Impairment of Systolic Ca^{2+} Handling

To test the relevance of oxidative stress and CaMKII for impaired systolic Ca^{2+} handling in AF/upon AF-simulation, measurements of Ca^{2+} cycling (epifluorescence microscopy, Fura-2) were performed in iPSC-CM after chronic AF-simulation (7 days). CaMKII was inhibited using AIP (1 µmol/L). N-acetylcysteine (NAC, 200 µmol/L) was used as ROS-scavenger. After 7 days of AF-simulation, iPSC-CM exhibited a diminished systolic Ca^{2+} transient amplitude (n=67 cardiomyocytes/3 differentiations/2 donors) compared with control (n=70/3/2). In contrast, Ca^{2+} transient amplitude was preserved in iPSC-CM after AF-simulation when concomitantly treated with either AIP (n=68/3/2) or NAC (n=80/3/2, Figure 7A and 7B). Diastolic Ca^{2+} and Ca^{2+} transient kinetics were not statistically different upon AF-simulation (Figure 7C through 7E). Sarcoplasmic reticulum Ca^{2+} load was decreased after AF-simulation, which could also be prevented by either inhibiting CaMKII or ROS scavenging (Figure 7F and 7G). Therefore, CaMKII and ROS might be one mechanism associated with the AF-induced impairment of cardiomyocyte Ca^{2+} cycling.

DISCUSSION

This study investigated the effects and mechanisms of AF on ventricular function. Patients with preserved LV function and AF showed no structural remodeling with

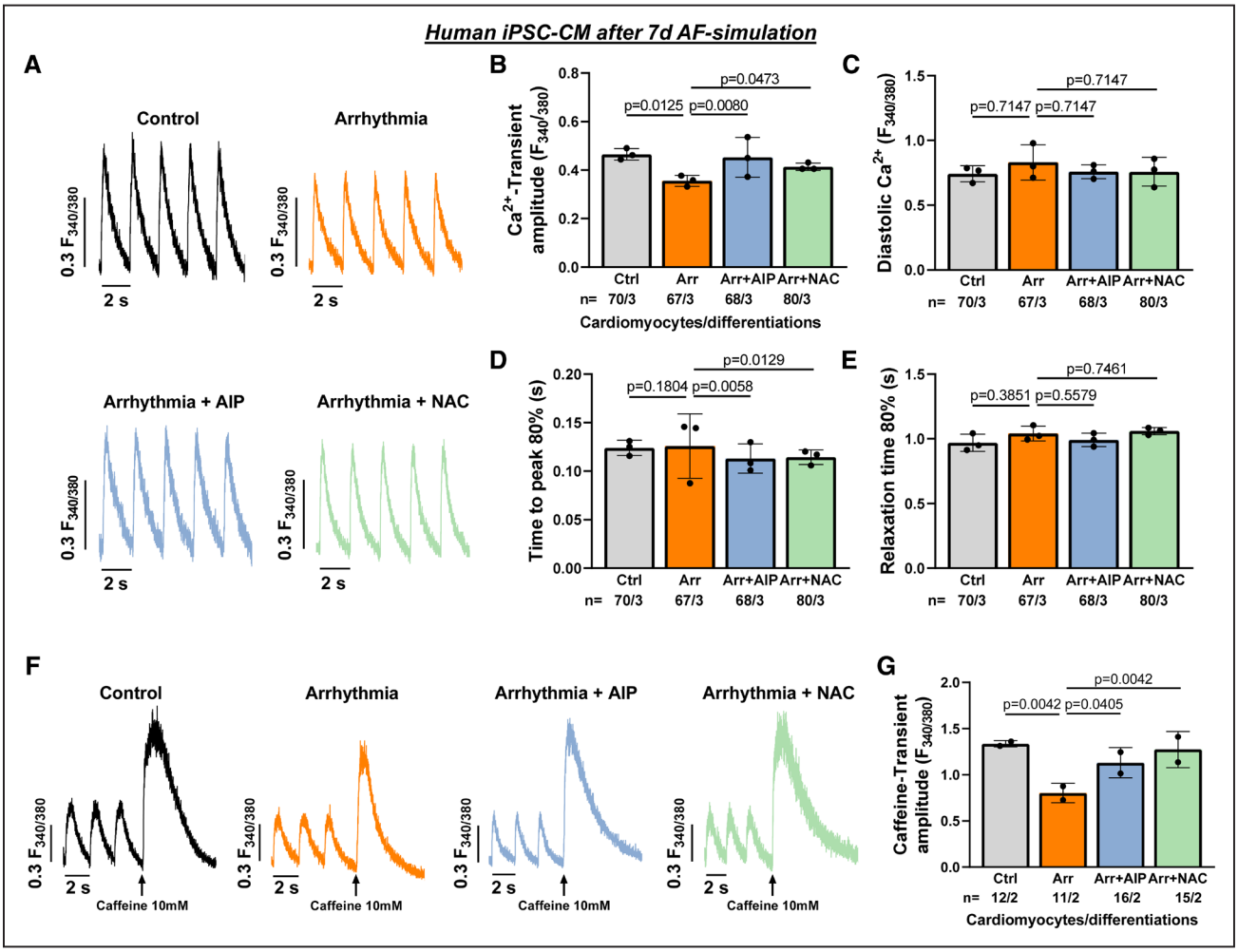

Figure 7. Effects of CaMKII and oxidative stress on Ca^{2+} handling after atrial fibrillation (AF)-simulation.
Human induced pluripotent stem cell cardiomyocytes (iPSC-CM) after chronic (7 d) AF-simulation (arrhythmic pacing: Arr; 60 bpm, 40% beat-to-beat-variability) or rhythmic pacing (control [Ctrl]; 60 bpm) and effects of CaMKII inhibition (AIP [autocamtide-2-related inhibitory peptide], 1 µmol/L) or oxidative stress reduction (NAC [N-acetylcysteine], 200 µmol/L). **A**, Representative recordings of stimulated Ca^{2+} transients (epifluorescence microscopy, Fura-2) and (**B**) mean values for Ca^{2+} transient amplitude, (**C**) diastolic Ca^{2+} levels, (**D**) time to peak 80%, **(E)** relaxation time 80% of human iPSC-CM upon chronic AF-simulation (n=67 cardiomyocytes/3 differentiations/2 donors), rhythmic pacing (n=70/3/2), AF-simulation + AIP (n=68/3/2) or AF-simulation+NAC (n=80/3/2). **F**, Original recordings of caffeine-induced Ca^{2+} transients (10 mmol/L caffeine, epifluorescence microscopy, Fura-2) and (**G**) mean caffeine-transient amplitude indicating the sarcoplasmic reticulum Ca^{2+} load of iPSC-CM after chronic AF-simulation (n=11/2/2), rhythmic pacing (n=12/2/2), AF-simulation+AIP (n=16/2/2) or AF-simulation+NAC (n=15/2/2). Data are provided as scatter plot with mean±SD. Each data point is calculated as mean value of all cardiomyocytes per differentiation. *P* were calculated using nested 1-way ANOVA and corrected for multiple comparisons using Holm-Sidak test.

respect to LV fibrosis but marked alterations in cardiomyocyte Ca^{2+} homeostasis with reduced systolic Ca^{2+} release. This could be explained by a diminished sarcoplasmic reticulum Ca^{2+} load accompanied by an increased sarcoplasmic reticulum Ca^{2+} leak. Moreover, cytosolic Na^+ and I_{NaL} were elevated, thereby prolonging action potential duration. Oxidative stress, CaMKII oxidation, and CaMKII activity were found to be augmented in LV myocardium from patients with AF leading to RyR2 hyperphosphorylation. These mechanisms may contribute to the Ca^{2+} handling changes in the AF ventricle, which could be prospectively confirmed in cardiomyocytes upon in vitro AF-simulation.

As fibrosis is increased in the atria of patients with AF[34,35] and LV fibrosis may contribute to cardiac dysfunction, histology of human AF LV was studied. Blinded semiautomated quantification of LV collagen proportionate area showed no difference between LV myocardium from SR or AF patients. Previous preclinical data showed less or no effects of pacing-induced AF in animal models on LV fibrosis compared with atrial fibrosis, depending on the model studied.[13,36] Of note, dogs with pacing-induced AF showed that increased LV fibrosis is rather mediated by the tachycardic component of AF.[37] Clinical data from echocardiographic measurements in patients with AF or cardiac magnetic resonance imaging reported an augmented diffuse LV fibrosis in patients with AF.[38,39] However, since fibrosis is considered to be irreversible, the improvement in LV function after catheter ablation in patients with AF and concomitant HF observed in clinical trials is mechanistically unexplained.[4,40] In addition, the functional improvement of LV function after SR restoration in patients with AF and HF has been demonstrated to occur rapidly.[40] Therefore, rather functional and thus reversible mechanisms might be involved in the contractile recovery following rhythm restoration. Our data provide new mechanistic concepts on how AF might deteriorate LV function via arrhythmic excitation by altering human cardiomyocyte Ca^{2+} handling. In functional investigations of human LV cardiomyocytes from AS patients with preserved LV function, we observed a reduced Ca^{2+} transient amplitude in patients with AF compared to SR. These results were confirmed in LV cardiomyocytes from nonfailing donors with AF and also after 24-hour in vitro AF-simulation in LV cardiomyocytes from nonfailing donors. Previous studies of neonatal rat ventricular cardiomyocytes reported a lower Ca^{2+} transient amplitude after irregular pacing, which however was accompanied with an increased diastolic Ca^{2+}[19] and in another study with concomitant changes in Ca^{2+} transient kinetics.[18] However, EC-coupling is largely species-dependent, and human specimens are warranted for translational aspects. Therefore, we investigated human myocardium from patients with AF and utilized isolated cardiomyocytes for standardized in vitro confirmation. Based on our findings in different human tissues and cellular preparations, we propose that AF/normofrequent arrhythmia per se is associated with profound disturbances of cardiomyocyte EC-coupling. To comprehensively investigate the underlying phenotype in a standardized human model, we used human iPSC-CM for chronic AF-simulation as these cells are suitable for long-term culture. In line with our observations in patients with AF, 7 days of AF-simulation caused a depression in Ca^{2+} transient amplitude without significant effects on diastolic Ca^{2+} or Ca^{2+} transient kinetics. This could be explained by a reduced sarcoplasmic reticulum Ca^{2+} content as it was detected upon AF-simulation in iPSC-CM. SERCA2a protein expression and function were found to be reduced in AF/AF-simulation indicating an impaired Ca^{2+} reuptake to the sarcoplasmic reticulum, which has also been suggested in irregularly paced neonatal rat ventricular cardiomyocytes.[18] In addition, we found that RyR2 was markedly hyperphosphorylated at the CaMKII site S2814 in the LV of patients with AF, thereby increasing the open probability of the channel.[41] Indeed, diastolic sarcoplasmic reticulum Ca^{2+} leak was abnormally augmented after AF-simulation in iPSC-CM. The combination of both, RyR2-mediated Ca^{2+} leak and decreased SERCA2a expression likely explain the reduced ventricular Ca^{2+} transient amplitude in AF. As Ca^{2+} binds to troponin C for myofilament activation, the amplitude of the systolic Ca^{2+} transient strongly determines systolic force. Thus, the Ca^{2+} leak-mediated reduction in sarcoplasmic Ca^{2+} load and consecutive impairment of systolic Ca^{2+} release can deteriorate cardiac contractility and may contribute to HF remodeling with systolic and diastolic dysfunction.[31,42]

Cardiomyocyte Ca^{2+} and Na^+ homeostasis are closely intertwined via NCX, which was found to be increased in protein expression in the LV of patients with AF. We demonstrate that AF-simulation in iPSC-CM resulted in elevated cellular Na^+ levels possibly explained by NCX-mediated Ca^{2+} extrusion in exchange with Na^+ under conditions of an increased Ca^{2+} leak. This mechanism could contribute to the diminished Ca^{2+} transients and sarcoplasmic reticulum Ca^{2+} load.[43] In addition, I_{NaL} was enhanced, thereby further increasing Na^+ influx leading to a prolonged action potential duration after AF simulation. Altered Na^+ homeostasis together with prolonged action potentials constitute typical hallmarks of maladaptive electrophysiological remodeling in HF[44] and may therefore further deteriorate cardiomyocyte EC-coupling in the AF ventricle.

We elucidated the underlying mechanisms of dysregulated EC-coupling in the ventricle of patients with AF and demonstrated that CaMKII activity was augmented. This could be explained by increased CaMKII oxidation at the regulatory domain Met281/282, which activates CaMKII,[33] likely because of increased levels of oxidative stress in the AF LV. These observations could be confirmed in iPSC-CM after AF-simulation and, with respect to CaMKII oxidation, in human nonfailing

myocardium from patients with AF. In line with our findings of increased oxidative stress in response to AF, previous studies of rat cardiomyocytes showed elevated levels of oxidative stress and enhanced CaMKII phosphorylation after irregular pacing.[17] Enhanced oxidative stress has also been described in in vivo AF models, although with concomitant tachycardia.[45] The contribution of both, oxidative stress and CaMKII could be confirmed by the finding that either CaMKII inhibition or ROS scavenging ameliorated the AF-simulation-induced impaired Ca^{2+} handling. Thus, oxidation-dependent increase in CaMKII activity may serve as an explanation for the depressed EC-coupling in the AF ventricle.

Nevertheless, AF-mediated arrhythmic excitation may cause further ionic disturbances in cardiomyocyte sub- or nanodomains and could also affect other ion currents/channels. Thus, additional AF-mediated functional and structural remodeling of the ventricle is possible. In particular, the significance of the pathophysiological drivers in the AF-ventricle could also depend on disease entity, comorbidities, and other features. Accordingly, further studies on the causative role of oxidative stress and CaMKII activation as AF-mediated triggers for ventricular dysfunction are warranted.

AF is a highly prevalent arrhythmia and 20% to 30% of patients with AF suffer from systolic LV dysfunction.[2] Moreover, AF was discussed to be associated with an increased risk for sudden cardiac death possibly via HF-related complications.[46] In clinical practice, patients with AF are often successfully rate controlled. However, recent clinical studies demonstrated that also at normal ventricular rates AF may deteriorate LV function.[2,10,11]

Rhythm control strategies have been demonstrated to improve cardiovascular outcomes in patients with AF as shown in different clinical trials, particularly in the EAST-AFNET 4 trial and the CASTLE-AF trial.[5,6] In addition, different studies reported an improved LV function after AF ablation in patients with HF with reduced ejection fraction and AF.[4,5]

Although of high clinical relevance, the underlying pathophysiology of the effects of AF on the ventricle is poorly understood. On the contrary, the effects of AF in the atria are broadly characterized.[47] This study elucidated that normofrequent AF with arrhythmic ventricular excitation impairs LV EC-coupling. This finding may, at least in part, explain the potential development of LV dysfunction in patients suffering from AF. In our human-based approaches we found no statistical difference regarding fibrosis or apoptosis in response to AF. Thus, the functional ventricular phenotype in the AF ventricle could potentially be reversible upon SR restoration. Our data thus indicate that AF could rather be the cause for the deterioration of LV-function than the consequence of an occult cardiomyopathy.[48]

In conclusion, this study provides the first mechanistic characterization of the detrimental effects of AF on the human ventricle and may pave the way to understand AF as a disease of the whole heart.

ARTICLE INFORMATION

Received June 21, 2021; revision received February 8, 2022; accepted February 14, 2022.

Affiliations

Department of Internal Medicine II, University Hospital Regensburg, Regensburg, Germany (S.P., M.K., T.S., M.P., T.K., A.P., L.S.M., S. Sossalla). Clinic for Cardiology and Pneumology, Georg-August University Göttingen, and DZHK (German Centre for Cardiovascular Research), partner site Göttingen, Germany (M.K., F.A., B.W., N.D., G.H., K.S.-B., S. Sossalla). Institut für Forschung und Lehre (IFL), Department of Molecular and Experimental Cardiology and Department of Cardiology, St. Josef-Hospital, Ruhr University Bochum, Germany (M.S., M.H., N.H.). Institute of Pathology, University Hospital Regensburg, Germany (F.B., C.B.). Department of Cardiology, Medical University of Graz, Austria (S.L.-H., S. Sedej, D.S.). Institute of Experimental Cardiovascular Research, University Medical Centre Hamburg-Eppendorf, Germany (C.E.M.). Department of Cardiothoracic Surgery, University Hospital Regensburg, Germany (D.C., C.S.). Department of Internal Medicine I, University of Würzburg, Germany (T.H.F.). Faculty of Medicine, University of Maribor, Maribor, Slovenia (S. Sedej). BioTechMed Graz, Graz, Austria (S. Sedej). Institute of Pharmacology and Toxicology, University of Würzburg, Germany (K.S.-B.).

Acknowledgments

We gratefully acknowledge the technical assistance of D. Riedl, J. Heine and Y. Metz. The heart image in the graphical abstract is licensed by Shutterstock.com/Usama Nasir MD.

Sources of Funding

K. Streckfuss-Bömeke and S. Sossalla are funded by the Deutsche Forschungsgemeinschaft (DFG) through the research grant SO 1223/4-1 and the F. Thyssen Foundation (Az 10.19.2.026MN). S. Pabel and T. Stehle are funded by the Else-Kröner-Fresenius Stiftung. S. Pabel is funded by the German Society of Internal Medicine. M. Knierim is supported by a research grant from the German Cardiac Society. B. Wenner is supported by the Göttinger Promotionskolleg, funded by the Else-Kröner-Fresenius-Stiftung. S. Sedej and S. Holzer are supported by the Austrian Science Fund (FWF; through grants I3301 and V-530). C. E. Molina is supported by the DFG (ES 569/2-1). G. Hasenfuß is funded by the DFG (SFB 1002). N. Hamdani is supported by the DFG (HA 7512/2-1 and HA 7512/2-4).

Disclosures

None.

REFERENCES

1. Benjamin EJ, Wolf PA, D'Agostino RB, Silbershatz H, Kannel WB, Levy D. Impact of atrial fibrillation on the risk of death: the Framingham Heart Study. *Circulation.* 1998;98:946–952. doi: 10.1161/01.cir.98.10.946
2. Sossalla S, Vollmann D. Arrhythmia-induced cardiomyopathy. *Dtsch Arztebl Int.* 2018;115:335–341. doi: 10.3238/arztebl.2018.0335
3. Anter E, Jessup M, Callans DJ. Atrial fibrillation and heart failure: treatment considerations for a dual epidemic. *Circulation.* 2009;119:2516–2525. doi: 10.1161/CIRCULATIONAHA.108.821306
4. Wang TJ, Larson MG, Levy D, Vasan RS, Leip EP, Wolf PA, D'Agostino RB, Murabito JM, Kannel WB, Benjamin EJ. Temporal relations of atrial fibrillation and congestive heart failure and their joint influence on mortality: the Framingham Heart Study. *Circulation.* 2003;107:2920–2925. doi: 10.1161/01.CIR.0000072767.89944.6E
5. Marrouche NF, Brachmann J, Andresen D, Siebels J, Boersma L, Jordaens L, Merkely B, Pokushalov E, Sanders P, Proff J, et al; CASTLE-AF Investigators. Catheter ablation for atrial fibrillation with heart failure. *N Engl J Med.* 2018;378:417–427. doi: 10.1056/NEJMoa1707855
6. Kirchhof P, Camm AJ, Goette A, Brandes A, Eckardt L, Elvan A, Fetsch T, van Gelder IC, Haase D, Haegeli LM, et al; EAST-AFNET 4 Trial Investigators. Early rhythm-control therapy in patients with atrial fibrillation. *N Engl J Med.* 2020;383:1305–1316. doi: 10.1056/NEJMoa2019422

7. Willems S, Meyer C, de Bono J, Brandes A, Eckardt L, Elvan A, van Gelder I, Goette A, Gulizia M, Haegeli L, et al. Cabins, castles, and constant hearts: rhythm control therapy in patients with atrial fibrillation. *Eur Heart J*. 2019;40:3793–3799c. doi: 10.1093/eurheartj/ehz782
8. Brignole M, Pentimalli F, Palmisano P, Landolina M, Quartieri F, Occhetta E, Calò L, Mascia G, Mont L, Vernooy K, et al. Corrigendum to: AV junction ablation and cardiac resynchronization for patients with permanent atrial fibrillation and narrow QRS: the APAF-CRT mortality trial. *Eur Heart J*. 2021;42:4768. doi: 10.1093/eurheartj/ehab669
9. Packer DL, Piccini JP, Monahan KH, Al-Khalidi HR, Silverstein AP, Noseworthy PA, Poole JE, Bahnson TD, Lee KL, Mark DB; CABANA Investigators. Ablation versus drug therapy for atrial fibrillation in heart failure: results from the CABANA Trial. *Circulation*. 2021;143:1377–1390. doi: 10.1161/CIRCULATIONAHA.120.050991
10. Prabhu S, Taylor AJ, Costello BT, Kaye DM, McLellan AJA, Voskoboinik A, Sugumar H, Lockwood SM, Stokes MB, Pathik B, et al. Catheter ablation versus medical rate control in atrial fibrillation and systolic dysfunction: the CAMERA-MRI Study. *J Am Coll Cardiol*. 2017;70:1949–1961. doi: 10.1016/j.jacc.2017.08.041
11. Hunter RJ, Berriman TJ, Diab I, Kamdar R, Richmond L, Baker V, Goromonzi F, Sawhney V, Duncan E, Page SP, et al. A randomized controlled trial of catheter ablation versus medical treatment of atrial fibrillation in heart failure (the CAMTAF trial). *Circ Arrhythm Electrophysiol*. 2014;7:31–38. doi: 10.1161/CIRCEP.113.000806
12. Gopinathannair R, Etheridge SP, Marchlinski FE, Spinale FG, Lakkireddy D, Olshansky B. Arrhythmia-induced cardiomyopathies: mechanisms, recognition, and management. *J Am Coll Cardiol*. 2015;66:1714–1728. doi: 10.1016/j.jacc.2015.08.038
13. Wijesurendra RS, Casadei B. Atrial fibrillation: effects beyond the atrium? *Cardiovasc Res*. 2015;105:238–247. doi: 10.1093/cvr/cvv001
14. Clark DM, Plumb VJ, Epstein AE, Kay GN. Hemodynamic effects of an irregular sequence of ventricular cycle lengths during atrial fibrillation. *J Am Coll Cardiol*. 1997;30:1039–1045. doi: 10.1016/s0735-1097(97)00254-4
15. Kochiadakis GE, Skalidis EI, Kalebubas MD, Igoumenidis NE, Chrysostomakis SI, Kanoupakis EM, Simantirakis EN, Vardas PE. Effect of acute atrial fibrillation on phasic coronary blood flow pattern and flow reserve in humans. *Eur Heart J*. 2002;23:734–741. doi: 10.1053/euhj.2001.2894
16. Wasmund SL, Li JM, Page RL, Joglar JA, Kowal RC, Smith ML, Hamdan MH. Effect of atrial fibrillation and an irregular ventricular response on sympathetic nerve activity in human subjects. *Circulation*. 2003;107:2011–2015. doi: 10.1161/01.CIR.0000064900.76674.CC
17. Slawik J, Adrian L, Hohl M, Lothschütz S, Laufs U, Böhm M. Irregular pacing of ventricular cardiomyocytes induces pro-fibrotic signalling involving paracrine effects of transforming growth factor beta and connective tissue growth factor. *Eur J Heart Fail*. 2019;21:482–491. doi: 10.1002/ejhf.1392
18. Ling LH, Khammy O, Byrne M, Amirahmadi F, Foster A, Li G, Zhang L, dos Remedios C, Chen C, Kaye DM. Irregular rhythm adversely influences calcium handling in ventricular myocardium: implications for the interaction between heart failure and atrial fibrillation. *Circ Heart Fail*. 2012;5:786–793. doi: 10.1161/CIRCHEARTFAILURE.112.968321
19. Lenski M, Schleider G, Kohlhaas M, Adrian L, Adam O, Tian Q, Kaestner L, Lipp P, Lehrke M, Maack C, et al. Arrhythmia causes lipid accumulation and reduced glucose uptake. *Basic Res Cardiol*. 2015;110:40. doi: 10.1007/s00395-015-0497-2
20. Berisha F, Götz KR, Wegener JW, Brandenburg S, Subramanian H, Molina CE, Rüffer A, Petersen J, Bernhardt A, Girdauskas E, et al. cAMP imaging at ryanodine receptors reveals β2-Adrenoceptor driven arrhythmias. *Circ Res*. 2021;129:81–94. doi: 10.1161/CIRCRESAHA.120.318234
21. Borchert T, Hübscher D, Guessoum CI, Lam TD, Ghadri JR, Schellinger IN, Tiburcy M, Liaw NY, Li Y, Haas J, et al. Catecholamine-Dependent β-Adrenergic signaling in a pluripotent stem cell model of takotsubo cardiomyopathy. *J Am Coll Cardiol*. 2017;70:975–991. doi: 10.1016/j.jacc.2017.06.061
22. Tohyama S, Hattori F, Sano M, Hishiki T, Nagahata Y, Matsuura T, Hashimoto H, Suzuki T, Yamashita H, Satoh Y, et al. Distinct metabolic flow enables large-scale purification of mouse and human pluripotent stem cell-derived cardiomyocytes. *Cell Stem Cell*. 2013;12:127–137. doi: 10.1016/j.stem.2012.09.013
23. Pabel S, Wagner S, Bollenberg H, Bengel P, Kovács Á, Schach C, Tirilomis P, Mustroph J, Renner A, Gummert J, et al. Empagliflozin directly improves diastolic function in human heart failure. *Eur J Heart Fail*. 2018;20:1690–1700. doi: 10.1002/ejhf.1328
24. Mohamed BA, Hartmann N, Tirilomis P, Sekeres K, Li W, Neef S, Richter C, Zeisberg EM, Kattner L, Didié M, et al. Sarcoplasmic reticulum calcium leak contributes to arrhythmia but not to heart failure progression. *Sci Transl Med*. 2018;10:eaan0724. doi: 10.1126/scitranslmed.aan0724
25. Pabel S, Reetz F, Dybkova N, Shomroni O, Salinas G, Mustroph J, Hammer KP, Hasenfuss G, Hamdani N, Maier LS, et al. Long-term effects of empagliflozin on excitation-contraction-coupling in human induced pluripotent stem cell cardiomyocytes. *J Mol Med (Berl)*. 2020;98:1689–1700. doi: 10.1007/s00109-020-01989-6
26. Pabel S, Mustroph J, Stehle T, Lebek S, Dybkova N, Keyser A, Rupprecht L, Wagner S, Neef S, Maier LS, et al. Dantrolene reduces CaMKIIδC-mediated atrial arrhythmias. *Europace*. 2020;22:1111–1118. doi: 10.1093/europace/euaa079
27. Despa S, Islam MA, Pogwizd SM, Bers DM. Intracellular [Na+] and Na+ pump rate in rat and rabbit ventricular myocytes. *J Physiol*. 2002;539:133–143. doi: 10.1113/jphysiol.2001.012940
28. Pabel S, Ahmad S, Tirilomis P, Stehle T, Mustroph J, Knierim M, Dybkova N, Bengel P, Holzamer A, Hilker M, et al. Inhibition of NaV1.8 prevents atrial arrhythmogenesis in human and mice. *Basic Res Cardiol*. 2020;115:20. doi: 10.1007/s00395-020-0780-8
29. Kolijn D, Pabel S, Tian Y, Lódi M, Herwig M, Carrizzo A, Zhazykbayeva S, Kovács Á, Fülöp GÁ, Falcão-Pires I, et al. Empagliflozin improves endothelial and cardiomyocyte function in human heart failure with preserved ejection fraction via reduced pro-inflammatory-oxidative pathways and protein kinase Gα oxidation. *Cardiovasc Res*. 2021;117:495–507. doi: 10.1093/cvr/cvaa123
30. Hamdani N, Krysiak J, Kreusser MM, Neef S, Dos Remedios CG, Maier LS, Krüger M, Backs J, Linke WA. Crucial role for Ca2(+)/calmodulin-dependent protein kinase-II in regulating diastolic stress of normal and failing hearts via titin phosphorylation. *Circ Res*. 2013;112:664–674. doi: 10.1161/CIRCRESAHA.111.300105
31. Sossalla S, Fluschnik N, Schotola H, Ort KR, Neef S, Schulte T, Wittköpper K, Renner A, Schmitto JD, Gummert J, et al. Inhibition of elevated Ca2+/calmodulin-dependent protein kinase II improves contractility in human failing myocardium. *Circ Res*. 2010;107:1150–1161. doi: 10.1161/CIRCRESAHA.110.220418
32. Sossalla S, Wagner S, Rasenack EC, Ruff H, Weber SL, Schöndube FA, Tirilomis T, Tenderich G, Hasenfuss G, Belardinelli L, et al. Ranolazine improves diastolic dysfunction in isolated myocardium from failing human hearts–role of late sodium current and intracellular ion accumulation. *J Mol Cell Cardiol*. 2008;45:32–43. doi: 10.1016/j.yjmcc.2008.03.006
33. Erickson JR, Joiner ML, Guan X, Kutschke W, Yang J, Oddis CV, Bartlett RK, Lowe JS, O'Donnell SE, Aykin-Burns N, et al. A dynamic pathway for calcium-independent activation of CaMKII by methionine oxidation. *Cell*. 2008;133:462–474. doi: 10.1016/j.cell.2008.02.048
34. Sohns C, Marrouche NF. Atrial fibrillation and cardiac fibrosis. *Eur Heart J*. 2020;41:1123–1131. doi: 10.1093/eurheartj/ehz786
35. Dzeshka MS, Lip GY, Snezhitskiy V, Shantsila E. Cardiac fibrosis in patients with atrial fibrillation: mechanisms and clinical implications. *J Am Coll Cardiol*. 2015;66:943–959. doi: 10.1016/j.jacc.2015.06.1313
36. Dosdall DJ, Ranjan R, Higuchi K, Kholmovski E, Angel N, Li L, Macleod R, Norlund L, Olsen A, Davies CJ, et al. Chronic atrial fibrillation causes left ventricular dysfunction in dogs but not goats: experience with dogs, goats, and pigs. *Am J Physiol Heart Circ Physiol*. 2013;305:H725–H731. doi: 10.1152/ajpheart.00440.2013
37. Avitall B, Bi J, Mykytsey A, Chicos A. Atrial and ventricular fibrosis induced by atrial fibrillation: evidence to support early rhythm control. *Heart Rhythm*. 2008;5:839–845. doi: 10.1016/j.hrthm.2008.02.042
38. Shantsila E, Shantsila A, Blann AD, Lip GY. Left ventricular fibrosis in atrial fibrillation. *Am J Cardiol*. 2013;111:996–1001. doi: 10.1016/j.amjcard.2012.12.005
39. Ling LH, Kistler PM, Ellims AH, Iles LM, Lee G, Hughes GL, Kalman JM, Kaye DM, Taylor AJ. Diffuse ventricular fibrosis in atrial fibrillation: noninvasive evaluation and relationships with aging and systolic dysfunction. *J Am Coll Cardiol*. 2012;60:2402–2408. doi: 10.1016/j.jacc.2012.07.065
40. Müller-Edenborn B, Minners J, Allgeier J, Burkhardt T, Lehrmann H, Ruile P, Merz S, Allgeier M, Neumann FJ, Arentz T, et al. Rapid improvement in left ventricular function after sinus rhythm restoration in patients with idiopathic cardiomyopathy and atrial fibrillation. *Europace*. 2019;21:871–878. doi: 10.1093/europace/euz013
41. Wehrens XH, Lehnart SE, Reiken SR, Marks AR. Ca2+/calmodulin-dependent protein kinase II phosphorylation regulates the cardiac ryanodine receptor. *Circ Res*. 2004;94:e61–e70. doi: 10.1161/01.RES.0000125626.33738.E2

42. Fischer TH, Maier LS, Sossalla S. The ryanodine receptor leak: how a tattered receptor plunges the failing heart into crisis. *Heart Fail Rev.* 2013;18:475–483. doi: 10.1007/s10741-012-9339-6
43. Schillinger W, Fiolet JW, Schlotthauer K, Hasenfuss G. Relevance of Na+-Ca2+ exchange in heart failure. *Cardiovasc Res.* 2003;57:921–933. doi: 10.1016/s0008-6363(02)00826-x
44. Dybkova N, Ahmad S, Pabel S, Tirilomis P, Hartmann N, Fischer TH, Bengel P, Tirilomis T, Ljubojevic S, Renner A, et al. Differential regulation of sodium channels as a novel proarrhythmic mechanism in the human failing heart. *Cardiovasc Res.* 2018;114:1728–1737. doi: 10.1093/cvr/cvy152
45. Goette A, Bukowska A, Lillig CH, Lendeckel U. Oxidative stress and microcirculatory flow abnormalities in the ventricles during atrial fibrillation. *Front Physiol.* 2012;3:236. doi: 10.3389/fphys.2012.00236
46. Waldmann V, Jouven X, Narayanan K, Piot O, Chugh SS, Albert CM, Marijon E. Association between atrial fibrillation and sudden cardiac death: pathophysiological and epidemiological insights. *Circ Res.* 2020;127:301–309. doi: 10.1161/CIRCRESAHA.120.316756
47. Staerk L, Sherer JA, Ko D, Benjamin EJ, Helm RH. Atrial fibrillation: epidemiology, pathophysiology, and clinical outcomes. *Circ Res.* 2017;120:1501–1517. doi: 10.1161/CIRCRESAHA.117.309732
48. Wijesurendra RS, Liu A, Eichhorn C, Ariga R, Levelt E, Clarke WT, Rodgers CT, Karamitsos TD, Bashir Y, Ginks M, et al. Lone atrial fibrillation is associated with impaired left ventricular energetics that persists despite successful catheter ablation. *Circulation.* 2016;134:1068–1081. doi: 10.1161/CIRCULATIONAHA.116.022931